発表者氏名	論文タイトル名	発表誌名	巻号	ページ	出版年
Mishima T, Ito Y, Hosono K, Tamura Y, Uchida Y, Hirata M, Suzuki T, Amano H, Kato S, Kurihara Y, Kurihara H, Hayashi I, Watanabe M, Majima M.	Calcitonin gene-related peptide facilitates revascularization during hindlimb ischemia in mice.	*Am. J. Physiol. Heart Circ. Physiol.*	300	H431-439	2010
Arima S*, Nishiyama K*, Ko T, Arima Y, Hakozaki Y, Sugihara K, Koseki H, Uchijima Y, Kurihara Y, Kurihara H. *These authors contributed equally to this work.	Angiogenic morphogenesis driven by dynamic and heterogeneous collective endothelial cell movement.	*Development.*	138	4763-4776	2011
Kitazawa T, Sato T, Nishiyama K, Asai R, Arima Y, Uchijima Y, Kurihara Y, Kurihara H.	Identification and developmental analysis of endothelin receptor type-A expressing cells in the mouse kidney.	*Gene Expr. Patterns.*	11	371-377	2011
Tonami K, Kurihara Y, Arima S, Nishiyama K, Uchijima Y, Asano T, Sorimachi H, Kurihara H.	Calpain 6, a microtubule-stabilizing protein, regulates Rac1 activity and cell motility through interaction with GEF-H1.	*J. Cell Sci.*	124	1214-1223	2011
Ando K, Takahashi M, Yamagishi T, Miyagawa-Tomita S, Imanaka-yoshida K, Yoshida T, Nakajima Y.	Tenascin C may regulate the recruitment of smooth muscle cells during coronary artery development.	*Differentiation*	81	299-306	2011
Obayashi K, Miyagawa-Tomita S, Matsumoto H, Koyama H, Nakanishi T, Hirose H.	Effects of transforming growth factor-β3 and matrix metalloproteinase-3 on the pathogenesis of chronic mitral valvular disease in dogs.	*Am J Vet Res*	72	194-202	2011
Kudo Y, Kaneko M, Nakazawa M, Tomita S.	A case of Cor Triatriatum with an abnormal P wave: The pacemaker action from the specialized tissue in the abnormal septum.	*Pediatric Cardiology*	32	1244-1248	2011
Kushiyama A, Okubo H, Sakoda H, Kikuchi T, Fujishiro M, Sato H, Kushiyama S, Iwashita M, Nishimura F, Fukushima T, Nakatsu Y, Kamata H, Kawazu S, Higashi Y, Kurihara H, Asano T.	Xanthine Oxidoreductase Is Involved in Macrophage Foam Cell Formation and atherosclerosis development.	*Arterioscler Thromb Vasc Biol.*	32	291-298	2012

Transcriptional Coactivator with PDZ-binding Motif Is Essential for Normal Alveolarization in Mice

Akihisa Mitani[1,2], Takahide Nagase[1], Kazunori Fukuchi[3], Hiroyuki Aburatani[4], Ryosuke Makita[2], and Hiroki Kurihara[2]

[1]Department of Respiratory Medicine and [2]Department of Physiological Chemistry and Metabolism, Graduate School of Medicine, University of Tokyo, Tokyo; [3]Bioscience Division II, Discovery Research Laboratories, Kyorin Pharmaceutical Company, Nogi, Tochigi; and [4]Genome Science Division, Research Center for Advanced Science and Technology, University of Tokyo, Tokyo, Japan

Rationale: **Transcriptional coactivator with PDZ-binding motif (TAZ) is assumed to act as a coactivator of several transcription factors including smad2/3. In the lung, *surfactant protein C* (*Sftpc*) is known to be a downstream target of thyroid transcription factor-1 (TTF-1)–TAZ transcriptional coactivation.**

Objectives: **The lung phenotype of *Taz*-deficient mice was explored.**

Methods: ***Taz*-deficient mice were analyzed pathologically and physiologically. Next, we performed microarray analysis to determine the genes closely related to abnormal lung development. Finally, *Taz*-heterozygous mice were injected with bleomycin.**

Measurements and Main Results: ***Taz*-deficient homozygotes showed abnormal alveolarization during lung development, which caused in adult mice airspace enlargement mimicking emphysema. There was no significant difference in the expression of *Sftpc* between wild-type and *Taz*-deficient lungs. Instead, microarray analysis identified some candidate downstream genes related to the pathogenesis, including the *connective tissue growth factor* (*Ctgf*) gene, which is required for normal lung development. *In vitro* studies showed that TAZ up-regulated *Ctgf* expression not only by reinforcing transforming growth factor-β/smad signals, but also by interfering in the more proximal *Ctgf* promoter region (from bp −123 to −76), defined as the TAZ response element. Furthermore, *Taz*-heterozygous mice were resistant to bleomycin-induced lung fibrosis.**

Conclusions: **The results indicate the importance of TAZ in lung alveolarization and its involvement in the pathogenesis of lung fibrosis.**

Keywords: *Taz*-deficient mice; emphysema; lung development; pulmonary fibrosis; connective tissue growth factor

Transcriptional coactivator with PDZ-binding motif (TAZ), also known as WW-domain containing transcription regulator-1 (Wwtr1), was originally identified as a 14-3-3–interacting protein (1). TAZ can act as a modulator of various transcription factors, including core-binding factor-1 (Cbfa1)/runt-related transcription factor-2 (Runx2) (2), thyroid transcription factor-1 (TTF-1) (3), paired box gene-3 (Pax3) (4), and smad2/3 (5). The C terminus of TAZ not only interacts directly with core transcriptional machinery to stimulate gene expression, but is also required for its localization to the membrane, suggesting that TAZ is involved in transmission of signals from the membrane and actin cytoskeleton to the nucleus (6). It has been reported that TAZ plays a role in smad nucleocytoplasmic shuttling (5).

To investigate the physiological role of TAZ, we generated *Taz*-knockout mice. Gene inactivation of *Taz* in mice resulted in pathological changes in the kidney and the lung (7–9). $Taz^{lacZ/lacZ}$ kidneys showed corticomedullary multicystic formation, somewhat reminiscent of human polycystic kidney disease, and severe concentrating defects (7).

Previous studies detected TAZ in embryonic lung epithelial cells (3). TAZ directly interacts with TTF-1, which is required for lung development and differentiation of peripheral respiratory epithelial cells, to activate the transcription of target genes including the surfactant proteins. In the presence of TTF-1, TAZ synergistically activates the expression of mouse *Sftpc-luciferase* reporter constructs (3).

Here, we show that TAZ deficiency caused lung developmental abnormalities, which led to an adult lung phenotype that resembled human emphysema, a common pathological feature of chronic obstructive pulmonary disease. We also identified connective tissue growth factor (CTGF), which is involved in epithelial-to-mesenchymal cell transition (10), lung fibrosis (11, 12), and lung development, as a downstream target of TAZ. Interestingly, *Taz*-heterozygous mice were resistant to bleomycin-induced lung fibrosis.

AT A GLANCE COMMENTARY

Scientific Knowledge on the Subject

TAZ (transcriptional coactivator with PDZ-binding motif) is a factor critical for lung alveolarization, and connective tissue growth factor (CTGF) may be involved in this process. *In vitro* studies have shown that TAZ up-regulates *Ctgf* expression not only by reinforcing TGF-β/smad signals, but also by interfering with the more proximal *Ctgf* promoter region. Furthermore, *Taz*-heterozygous mice are resistant to bleomycin-induced lung fibrosis.

What This Study Adds to the Field

This study shows that TAZ is an important factor in lung alveolarization and is involved in the pathogenesis of lung fibrosis.

METHODS

Animals

Taz-deficient mice were generated as described previously (7). Mice for the bleomycin-induced fibrosis model had been backcrossed to the C57BL6/J strain for more than nine generations. All experiments were

(*Received in original form December 5, 2008; accepted in final form June 3, 2009*)

Supported by a grant-in-aid for Scientific Research from the Ministry of Education, Science, Sports, Culture, and Technology of Japan; a grant to the Respiratory Failure Research Group from the Ministry of Health, Labor, and Welfare, Japan; a grant-in-aid for Comprehensive Research on Aging and Health from the Ministry of Health, Labor, and Welfare, Japan; and the Global COE Program (Integrative Life Science Based on the Study of Biosignaling Mechanisms), MEXT, Japan.

Correspondence and requests for reprints should be addressed to Takahide Nagase, M.D., Ph.D., Department of Respiratory Medicine, Graduate School of Medicine, University of Tokyo, Hongo 7-3-1, Bunkyo-ku, Tokyo 113-0033, Japan. E-mail: takahide-tky@umin.ac.jp

This article has an online supplement, which is accessible from this issue's table of contents at www.atsjournals.org

Am J Respir Crit Care Med Vol 180. pp 326–338, 2009
Originally Published in Press as DOI: 10.1164/rccm.200812-1827OC on June 4, 2009
Internet address: www.atsjournals.org

approved by the Ethics Committee for Animal Experiments (University of Tokyo, Tokyo, Japan). The day that the vaginal plug was found was considered to be embryonic day 0.5 (E0.5); and the day of birth, as postnatal day 0 (P0).

For bleomycin treatment, 9- to 10-week-old mice were treated for 10 days with intraperitoneal injections, at 10 mg/kg per day, of bleomycin sulfate (Nippon Kayaku Co., Tokyo, Japan) dissolved in sterile saline. They were killed at 28 days, after completing the last injection.

Histological and Physiological Analysis

The lungs were fixed by intratracheal injection of 10% buffered formalin at a constant pressure of 25 cm H_2O for at least 24 hours. As for embryonic lungs, the intact thorax was immersed in 4% buffered paraformaldehyde. Specimens were paraffin embedded, cut into 14-μm-thick sections, and stained with hematoxylin–eosin (H&E) or elastica van Gieson or Masson trichrome staining.

The mean linear intercept, as a measure of interalveolar wall distance, was calculated by the Thurlbeck method (13). Briefly, lines were drawn across light microscopic images of the lung section stained with hematoxylin–eosin. Then, the mean linear intercept was calculated by dividing the total length of the line by the total number of intercepts encountered in 72 lines per each lung. The destructive index was calculated to evaluate the destruction of the alveolar wall according to the method described previously (14). Fifty randomly selected fields in each section were used to measure the destructive index. The Ashcroft score was counted as described previously (15). A paraffin section of lung was systematically scanned in a microscope and each successive field was individually assessed for severity of interstitial fibrosis and allotted a score, using a predetermined scale of severity. The mean score of 40 fields was taken as the fibrosis score.

Physiological Analysis

Lung elastance of *Taz*-homozygous mice was measured as described previously (16). Anesthetized mice were mechanically ventilated (model 683; Harvard Apparatus, South Natick, MA). After the chest was widely opened, tracheal pressure and tracheal flow were measured with a piezoresistive microtransducer (8510B-2; Endevco, San Juan Capistrano, CA) and a Fleisch pneumotachograph (model 00000; Metabo SA, Lausanne, Switzerland), respectively. For lung elastance of *Taz*-heterozygous mice, the flexiVent ventilator (Scireq, Montreal, PQ, Canada) was also used. To construct the pressure–volume curve, we used open-chest mice. Using a syringe attached to a three-way stopcock, air was instilled until the lungs were inflated to total lung capacity (transpulmonary pressure, <26 cm H_2O). The lungs were then subsequently deflated. After each 0.1-ml deflation, the three-way stopcock was adjusted so that the pressure in the system could be measured. A 30-second pause was observed between each volume change to ensure that no leaks were present in the system.

Quantitative Real-time Reverse Transcription-Polymerase Chain Reaction

Quantitative real-time reverse transcription-polymerase chain reaction (RT-PCR) was performed with the LightCycler system (Roche Diagnostics, Mannheim, Germany) according to the protocol provided by the manufacturer. Sequences of the primers are available on request. Quantification was performed in duplicate and normalized to *Gapdh* mRNA level.

Gene Chip Experiment

Total RNAs from E15.5 lungs were extracted with an RNeasy mini kit (Qiagen, Hilden, Germany). Equal amounts of total RNA from four *Taz*-deficient lungs and four wild-type lungs were mixed and subjected to the mouse genome 430 2.0 array (900496; Affymetrix, Santa Clara, CA). The hybridized arrays were scanned and analyzed with the Affymetrix Gene Chip system. Decreased genes were defined as those with at least a −0.6-fold decrease in mRNA content. Up-regulated genes were defined as those with a greater than 0.6-fold increase.

Immunohistochemistry and Western Blotting

For immunohistochemistry, tissue sections were processed for epitope retrieval by incubation in sodium citrate buffer (10 mM sodium citrate; pH 6.0). Antibodies against CTGF (ab6992; Abcam, Cambridge, UK) and smad3 (sc-8332; Santa Cruz Biotechnology, Santa Cruz, CA) were used. smad3-positive nuclei were counted until the total nuclei count reached more than 500 per one slide (n = 8). For Western blotting, lung lysates were fractioned, transferred onto nitrocellulose membranes, and probed with anti-CTGF (sc-14939; Santa Cruz Biotechnology), anti-β-actin (A5441; Sigma-Aldrich, St. Louis, MO), and suitable horseradish peroxidase-conjugated secondary antibodies.

5-Bromo-4-chloro-3-indolyl-β-D-galactopyranoside Staining

LacZ expression was detected by staining with 5-bromo-4-chloro-3-indolyl-β-D-galactopyranoside (X-Gal) for β-galactosidase activity. Whole lungs were fixed in 0.1 M phosphate buffer (pH 7.3) containing 0.2% glutaraldehyde, 5 mM ethyleneglycol-*bis*-(β-aminoethyl ether)-*N,N'*-tetraacetic acid, and 2 mM $MgCl_2$. Samples were then incubated overnight at 30°C in 0.1 M phosphate buffer containing 2 mM $MgCl_2$, 0.02% Nonidet P-40, 0.01% sodium deoxycholate, 5 mM potassium ferrocyanide, 5 mM potassium ferricyanide, and X-Gal (2 mg/ml). After staining, some samples were cryosectioned at 14 μm and photographed.

Cell Culture and Dual-Luciferase Reporter Assay

To investigate the role of TAZ as a transcriptional coactivator *in vitro*, *Taz* mRNA was knocked down or overexpressed in LA4 cells (immortalized lung epithelial cells). Furthermore, we used a dual-luciferase reporter assay to examine the interaction between the *Ctgf* promoter lesion and TAZ.

LA4 cells were grown in Ham's F12K medium containing 15% fetal bovine serum. In some studies, transforming growth factor (TGF)-β_1 at 0.5–10 ng/ml (R240-B/CF; R&D Systems, Inc., Minneapolis, MN) and/or 10 μM LY364947 (Sigma-Aldrich) was added.

Stealth small interfering RNAs (siRNAs) against *Taz* (*Taz*-994, -1235, and -1378) were synthesized and purified by Invitrogen (Carlsbad, CA). Sequences are as follows: forward *Taz*-994, 5′-AAUCCUCUCUCUCCAUCUGGAUC-3′; and reverse *Taz*-994, 5′-GAUCCAGAUGGAGAGAGAGAGGAUU-3′. Stealth RNAi negative control medium GC duplex (Invitrogen) was used as a negative control. LA4 cells were transfected with RNAiMAX (Invitrogen).

Full-length *Taz* cDNA was cloned into pcDNA3 (Invitrogen). The 5′-flanking region of the *Ctgf* gene was cloned into the pGL3-Basic vector (Promega, Madison, WI) and pLuc-MCS vector (Stratagene, La Jolla, CA) to form the *Ctgf* promoter-luciferase reporter construct. LA4 cells were transfected with these plasmids, using Lipofectamine 2000 (Invitrogen). The activities of firefly luciferase in pGL3/pLuc and *Renilla* luciferase in pRL-SV40 were determined according to the dual-luciferase reporter assay protocol recommended by Promega.

Data Analysis

All data are expressed as means ± SEM unless otherwise stated. Differences between experimental groups were examined for statistical significance by the Student *t* test or Mann-Whitney rank sum test. A *P* value less than 0.05 denoted the presence of statistical significance. Statistical analyses were performed with SigmaStat (version 3.5; Systat Software, Chicago, IL).

RESULTS

Emphysema-like Phenotype of *Taz*-homozygous Adult Mice

To determine whether the absence of TAZ expression leads to structural abnormalities, lung morphology of 9-month-old *Taz* knockout mice was compared with that of their wild-type littermates. Viewed from an open abdomen, $Taz^{lacZ/lacZ}$ lungs pushed the diaphragm caudally, and after extirpation and fixation with 10% formalin at a constant pressure of 25 cm H_2O, they appeared clearly larger and somewhat paler than wild-type lungs (Figures 1A and 1B). Next, we examined the

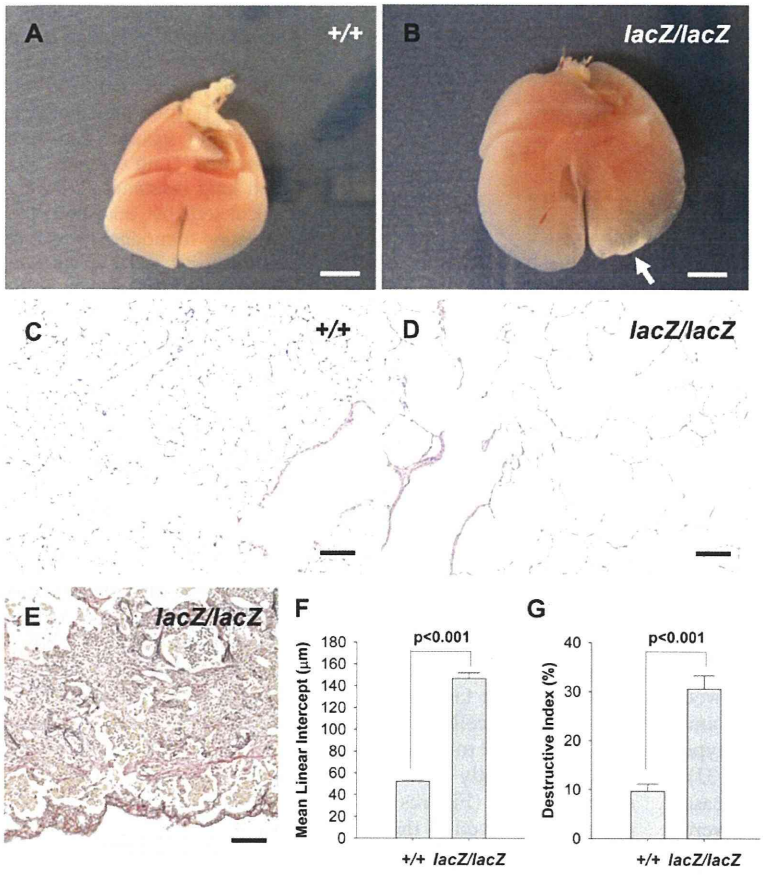

Figure 1. Morphometric analysis of *Taz*-deficient mice aged 9 months. *Scale bars*: (*A* and *B*) 5 mm; (*C–E*) 100 μm. (*A* and *B*) Gross appearance of $Taz^{+/+}$ and $Taz^{lacZ/lacZ}$ lungs after fixation. Some $Taz^{lacZ/lacZ}$ mice had a white fibrotic change at the lung base (*arrow*). (*C* and *D*) Hematoxylin and eosin staining of lung sections of $Taz^{+/+}$ and $Taz^{lacZ/lacZ}$ mice. (*E*) Elastica van Gieson staining of a lower lung section of the mouse in (*B*). (*F* and *G*) Mean linear intercept (*F*) and destructive index (*G*) from lung sections of $Taz^{+/+}$ mice (n = 5) and $Taz^{lacZ/lacZ}$ mice (n = 5). Data represent means ± SEM.

lungs by light microscopy. There were no obvious morphological abnormalities in conducting airway epithelial cells at the level of light microscopy. However, enlargement of the alveolar space was noted across the entire *Taz*-deficient lungs and the alveolar walls were somewhat thin and fragile (Figures 1C and 1D). In two samples of the five *Taz*-deficient mice, focal areas of alveolar space filled with inflammatory cells (predominantly macrophages) were noted, together with fibrotic changes and alveolar wall disruption, similar to the histopathological changes seen in human emphysema (Figure 1E), although these changes occupied rather small areas (<0.5 and <5% of the whole lung, respectively).

To assess these emphysema-like changes more quantitatively, histomorphometric analysis was conducted. The mean linear intercept was significantly increased in *Taz*-deficient mice compared with wild-type mice (146.9 ± 5.3 vs. 52.1 ± 1.0 cm H_2O/ml; $P < 0.001$; Figure 1F). The destructive index was also significantly increased in *Taz*-knockout mice (30.6 ± 2.7 vs. 9.7 ± 1.4%; $P < 0.001$; Figure 1G). Focal areas with inflammation described previously were so small that they had almost no effect on the destructive index.

Next, bronchoalveolar lavage fluid (BALF) samples of younger (2-mo-old) $Taz^{lacZ/lacZ}$, $Taz^{+/lacZ}$, and wild-type mice were analyzed. At that age, no focal inflammatory regions were noted, in contrast to the 9-month-old mice, even in $Taz^{lacZ/lacZ}$ mice. However, the numbers of macrophages and lymphocytes in the BALF of *Taz*-deficient mice were significantly higher than those in heterozygous or wild-type mice (*see* Figures E1A and E1C in the online supplement), similar to that seen in some patients with emphysema. The number of neutrophils in BALF also tended to be higher, but was not statistically significant (*see* Figure E1B in the online supplement).

To characterize the emphysema-like phenotype of *Taz*-deficient mice, lung elastance was measured in 8-month-old *Taz*-deficient and wild-type mice (Figure 2A). A significant decrease in lung elastance was evident (8.4 ± 1.2 vs. 15.8 ± 0.7 cm H_2O/ml; $P < 0.001$). The deflation limbs of the pressure–volume curves showed markedly increased lung volumes at any pressure in mice lacking TAZ (Figure 2B). The air volume injected at 26 cm H_2O was significantly increased in *Taz*-deficient mice compared with their wild-type siblings (78.5 ± 3.6 vs. 30.6 ± 2.8 ml/kg; $P < 0.001$). These mechanical properties of the lung were consistent with the histological and morphometric properties, and emphasized the emphysema-like abnormality in *Taz*-knockout mice.

Emphysema-like Changes in *Taz*-deficient Mice Are Due to Abnormal Lung Development

Airspace enlargement is a major pathological feature of human emphysema, but the change is thought to be caused by disruption of fully developed alveoli. However, many genetically altered models assumed to mimic emphysema have been proved developmental abnormalities rather than destruction of mature lung tissue. Therefore, we histologically examined the developing lungs of control and $Taz^{lacZ/lacZ}$ mice at various developmental stages (Figure 3).

The lungs of the $Taz^{+/+}$ littermates developed normally from E16.5 to P14 (Figures 3A, 3C, 3E, and 3G). At E18.5, the terminal bronchioles opened into a smooth-walled channel dividing into several saccules (Figure 3C). After the formation

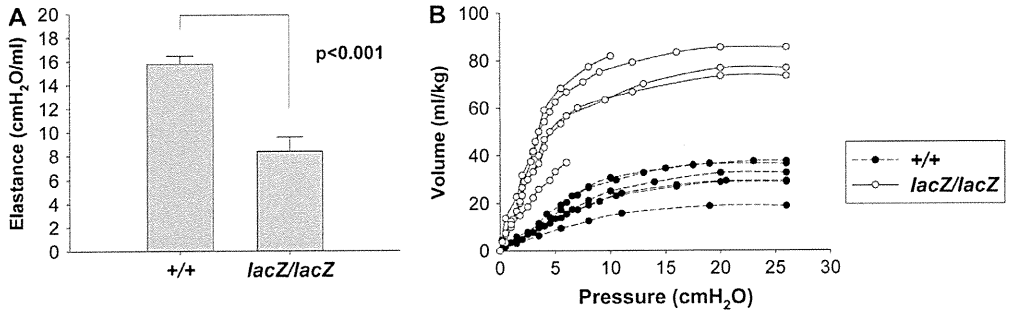

Figure 2. Physiological analysis of $Taz^{lacZ/lacZ}$ mice aged 7 months (n = 5) and wild-type siblings (n = 6). (*A*) Lung elastance. Tracheal pressure (Ptr), flow, and volume (V) were measured. Lung elastance (E_L) and lung resistance (R_L) were calculated by adjusting the equation of motion: $Ptr = E_L \cdot V + R_L(dV/dt) + K$, where K is a constant. (*B*) Deflation limbs of pressure–volume curves. Data are expressed as milliliters per kilogram of body weight.

of the secondary septa, the saccules transformed into alveolar ducts and alveolar sacs lined with alveoli by the end of the alveolar stage (Figures 3E and 3G). Once fully developed, $Taz^{+/+}$ lungs showed a slight increase in alveolar space (Figure 3K). Interestingly, most $Taz^{lacZ/lacZ}$ lungs grew normally until birth (Figures 3B and 3D), whereas some embryos had smaller and immature lungs than their wild-type littermates. After birth, the terminal airways were in close proximity to the pleural surface with larger airspace by P5 (Figure 3F). Since then, although the number of saccules increased in proportion to the whole lung size, enlarged airspace in $Taz^{lacZ/lacZ}$ lungs showed less alveolar compartmentalization than wild-type lungs, and the histological difference between $Taz^{lacZ/lacZ}$ and wild-type lungs became much clearer by 3 months (Figures 3H and 3J). The alveoli of $Taz^{lacZ/lacZ}$ lungs showed a further small increase in size by 9 months (Figure 3L). No inflammatory changes were noted from the embryonic stage to 3 months in both groups.

These results indicate that *Taz*-deficient mice have abnormalities in distal lung morphogenesis mainly during the saccular (E17 to P5) and alveolar (P5 to P14) stages, which lead to the emphysema-like phenotype in adult mice.

Normal Expression of TTF-1 Target Genes and Decreased Expression of Endothelial and Mesenchymal Marker Genes in *Taz*-deficient Mice

To investigate how deficiency of TAZ affects lung development, quantitative RT-PCR was performed on lung samples at E16.5, before *Taz*-deficient lungs begin to show histological changes relative to the wild-type control. TAZ is known to act as a coactivator of TTF-1 *in vitro* (3). First, we tested whether inadequate transcriptional activity of TTF-1 contributes to the lung phenotype of $Taz^{lacZ/lacZ}$ mice, because TTF-1 is essential for lung development (17). We determined the expression of *Ttf-1* and its target genes (*Sftpc, Clara cell secretory protein* [*Ccsp*], and *bone morphogenetic protein-4* [*Bmp4*]) by quantitative RT-PCR (Figure 4A). The results showed no significant differences in their expression between $Taz^{+/+}$ and $Taz^{lacZ/lacZ}$ lungs, although in the *Taz*-knockout lungs *Sftpc* and *Ccsp* transcripts tended to decrease slightly, which may be explained by differences in cell population and maturity rather than the direct effect on their transcription. When normalized with the mRNA level of *Ttf-1* instead of *Gapdh*, the results were almost the same (data not shown). Analysis of 8-week-old *Taz*-deficient lungs also showed no decrease in expression of the previously mentioned genes, except for *Bmp4* mRNA (Figure 4B). These results suggest that the role of TAZ as a coactivator of TTF-1 is not critical for embryonic and postnatal lung development.

We then measured the expression of various marker genes, including *E-cadherin* (*ECD*) (epithelial cells), *vascular endothelial growth factor receptor- 2* (*VEGFR-2, Flk-1*) (endothelial cells), *platelet-derived growth factor receptor-α* (*PDGFR-A*) (myofibroblasts), *α-smooth muscle actin* (*α-SMA*) (smooth muscle), and *vimentin* (mesenchymal cells) (Figures 4C and 4D). E16.5 *Taz*-deficient lungs had slightly decreased expression of *vimentin* mRNA and 8-week-old *Taz*-deficient lungs had markedly decreased expression of *Flk1* as well as *vimentin*. It was interesting that marker gene expression of endothelial cells and mesenchymal cells was decreased in the *Taz*-knockout lungs, although TAZ was expressed at epithelial cells.

Among various angiogenic factors, we focused on platelet-derived growth factor-α (PDGF-A). PDGF-A is expressed at lung epithelial cells and *PDGF-A* knockout mice have a similar lung phenotype to *Taz*-deficient mice (18). *PDGF-A* transcripts were significantly reduced in both embryonic and adult *Taz*-deficient lungs (Figures 4C and 4D), suggesting that PDGF-A might be involved in the pathogenesis of *Taz*-deficient lungs.

Microarray Analysis

We next performed microarray analysis with total RNA extracted from E15.5 $Taz^{+/+}$ and $Taz^{lacZ/lacZ}$ lungs (GEO accession number, GSE10805) to determine the genes closely related to abnormal lung development,. At that stage of development, lungs of *Taz*-deficient and wild-type mice were morphologically identical, as determined by optical microscopy. From the list of genes whose expression was decreased in *Taz*-deficient mice (*see* Table E1 in the online supplement), we first selected five genes: *metallothionein-1* and *-2* (*MT1* and *MT2*), *transmembrane-4 superfamily member-1* (*Tm4sf1*), *fibulin-5* (*Fbln5*), and *Ctgf*, considering the potential relationship of their function to lung development. The up-regulated genes are listed in Table E2 in the online supplement. Some of the genes are related to hemoglobin, and some are related to stress protein. But we could not find any genes possibly related to lung development.

MT1 and MT2 are involved in metalloregulatory processes that include cell growth and multiplication (19). Tm4sf1, also called the tumor-associated antigen L6 (TAL6), is expressed on most epithelial cell carcinomas and appears to be involved in cancer invasion and metastasis (20). Fbln5 is an essential determinant of elastic fiber organization and *Fbln5*-deficient mice exhibit a severely disorganized elastic fiber system throughout the body, including severe emphysema (21). CTGF is implicated in fibroblast proliferation, cellular adhesion, angiogenesis, and extracellular matrix deposition (22, 23) and CTGF deficiency causes pulmonary hypoplasia (24). In addition to these five genes, we selected *angiopoietin-like-4* (*Angptl4*) although its function is involved mainly in lipid metabolism. Because Angptl4 is controlled by TGF-β/smad signaling (25), we thought that TAZ might control *Angptl4* expression as a coactivator of smads.

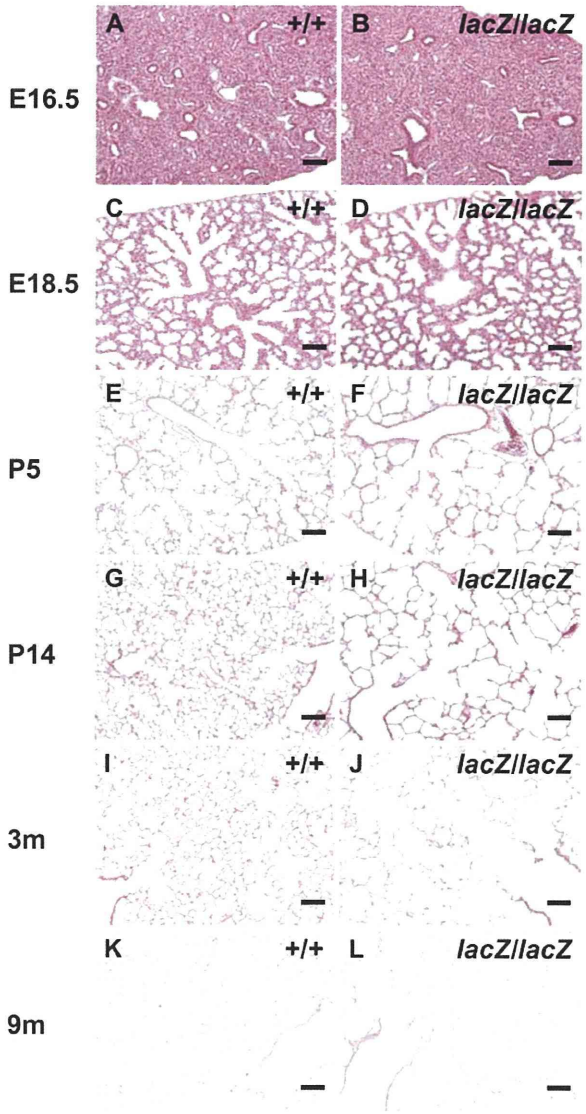

Figure 3. Histological examination of developing lungs in control (*A, C, E, G, I,* and *K*) and $Taz^{lacZ/lacZ}$ (*B, D, F, H, J,* and *L*) mice. *Scale bars*: 100 μm. E = embryonic day; P = postnatal day.

Decreased expression of all six genes was confirmed by quantitative RT-PCR using samples of E16.5 lungs (Figure 4E). In the adult lungs (Figure 4F), however, *MT1* and *MT2* expression was increased, rather than decreased, in *Taz*-deficient mice, although the difference was significant only in the case of *MT2*. The discrepancy in *MT1* and *MT2* expression in E16.5 and 2-month-old lungs could reflect processes of cellular damage and protective response during abnormal development caused by TAZ deficiency. *Fbln5* and *Ctgf* expression was significantly decreased in *Taz*-knockout mice, consistent with the microarray results. Fbln5 and CTGF are both related to the formation of extracellular matrix, which is important for alveolarization (26).

Close Relationship between TAZ and CTGF

To confirm the relationship between TAZ and the previously mentioned genes that had been picked up, we made use of LA4 cells, an immortalized lung epithelial cell line. Although they were derived from an alveolar epithelial cell, the expression of lung epithelial cell markers (*Ttf-1*, *Sftpc*, and *Ccsp*) was much less in LA4 cells than in whole lung (data not shown), which is a common characteristic of immortalized lung cell lines, such as A549 cells. On the other hand, *Taz* mRNA was expressed to almost the same extent both in LA4 cells and whole lung. Because the marker genes of differentiated lung epithelial cells, such as *Sftpc*, were not affected even in *Taz*-deficient lungs, we thought that use of the LA4 cell line could be permitted, recognizing its limitation.

PDGF-A and the six genes identified from the results of microarray analysis were all expressed in LA4 cells, and TAZ was depleted in LA4 cells by means of siRNA. LA4 cells depleted of TAZ, using *Taz*-994, grew in apparently the same manner as controls, and the mRNA from these cells was analyzed by quantitative RT-PCR. *Taz* mRNA was decreased to about one-fifth within 2 days in *Taz*-994–transfected cells (Figure 5A). Among all of the examined genes, mRNAs of *Tm4sf1*, *Fbln5*, and *Ctgf* showed down-regulation in *Taz*-deficient cells (Figure 5A), and time series analysis showed that only *Ctgf* mRNA was constantly reduced (*see* Figure E2 in the online supplement). The expression patterns of the other genes were not confirmative of the gene chip analysis. As for *Ctgf*, the mRNA levels were also decreased in cells transfected with another *Taz* siRNA (data not shown).

Next, *Taz* cDNA expression vectors were transfected into LA4 cells. *Taz* mRNA was overexpressed in the transfected cells. As expected, *Ctgf* mRNA was up-regulated in TAZ-overexpressing cells (Figure 5B). These results suggest a close relationship between TAZ and CTGF in lung epithelial cells.

Underexpression of CTGF in Embryonic Lungs of *Taz*-deficient Mice

Previous immunohistochemical studies reported that CTGF protein is expressed in distal airway epithelial cells of embryonic lungs (27) and in type 2 alveolar cells of adult lungs (12). Western blotting showed decreased CTGF expression in both embryonic and adult *Taz*-deficient lungs (Figure 6A). Immunohistochemical analysis of E18.5 wild-type lungs with anti-CTGF antibody showed staining of airway epithelial cells and parenchyma, the same as previously reported (Figure 6B). On the other hand, *Taz*-deficient lungs had much weaker staining than wild-type littermates (Figure 6C).

X-Gal staining of the $Taz^{lacZ/lacZ}$ lungs at the same stage, which reflected the site of TAZ expression during normal development, showed staining of the nuclei of bronchial epithelial cells and alveolar epithelial cells (Figure 6E), which is also the same pattern as previously reported (3). It was concluded that TAZ and CTGF expressed in almost the same distribution, although the immunohistochemical staining with anti-CTGF antibody was diffused because CTGF is a secreted protein.

Therefore, both TAZ and CTGF were expressed in bronchial epithelial cells and alveolar epithelial cells in wild-type mice, and CTGF expression was considerably reduced in *Taz*-knockout lungs.

TGF-β/smad Signals Are Not Absent in Developing *Taz*-deficient Lungs

TGF-β induces CTGF expression in many cell types because the *Ctgf* promoter contains a TGF-β response element (28). Furthermore, it has been reported that TAZ binds smad2/3–4 complexes and is recruited to TGF-β response elements on stimulation with TGF-β (5). Therefore, we postulated that TGF-β signal insufficiency might be the cause of the emphysema-like phenotype, especially because lung development is im-

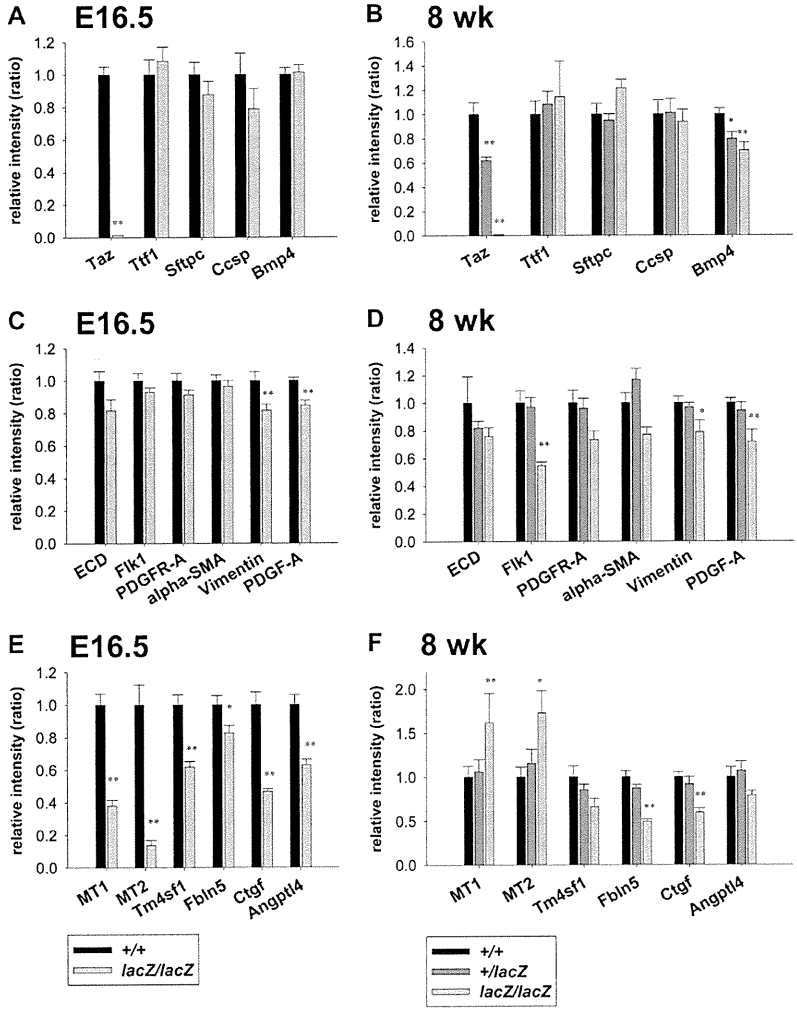

Figure 4. Quantitative real-time reverse transcription-polymerase chain reaction (RT-PCR) of (*A, C,* and *E*) embryonic day 16. 5 (E16.5) $Taz^{lacZ/LacZ}$ lungs (n = 10) versus their wild-type siblings (n = 12) and of (*B, D,* and *F*) 8-week-old wild-type (n = 9) versus $TAZ^{+/lacZ}$ (n = 13) versus $Taz^{lacZ/LacZ}$ mice (n = 4). (*A* and *B*) Transcriptional coactivator with PDZ-binding motif (TAZ)- and thyroid transcription factor-1 (TTF-1)–related genes. (*C* and *D*) Marker genes of various cell types and *PDGF-A.* (*E* and *F*) The six genes selected from the results of microarray analysis. *See* text for definition of gene abbreviations. Data represent means ± SEM. $*P < 0.05$, $**P < 0.01$.

paired in *smad3*-deficient mice (29, 30). Real-time RT-PCR revealed that there was no difference in *smad3* expression between *Taz*-deficient and wild-type lungs (Figures 7B and 7C). We then thought of the possibility that smad3 shuttling to nuclei was inhibited by TAZ deficiency. Immunohistochemistry with anti-smad3 antibody, however, revealed the presence of smad3 in the nucleoli of epithelial cells even in *Taz*-deficient lungs (Figure 7A). We counted the number of smad3-positive nuclei in wild-type and *Taz*-deficient mice. The rates were 12.9 ± 1.0 versus 10.1 ± 1.3%, respectively, and there was no significant difference, suggesting that smad3 signals were not completely blocked in *Taz*-deficient mice.

In addition to *Ctgf* and *Angptl4*, we selected three other target genes of TGF-β/smad signals that are known to be expressed in the lungs: *plasminogen activator inhibitor-1* (*PAI-1*) (31), *collagen type I α2* (*Col1a2*) (32), and *transgelin* (*Tagln*) (33). The expression levels of these three genes were not down-regulated to levels as low as *Ctgf* mRNA in E16.5 and 8-week-old lungs (Figures 7B and 7C). This is partly because TGF-β signal might not be essential for the expression of these genes.

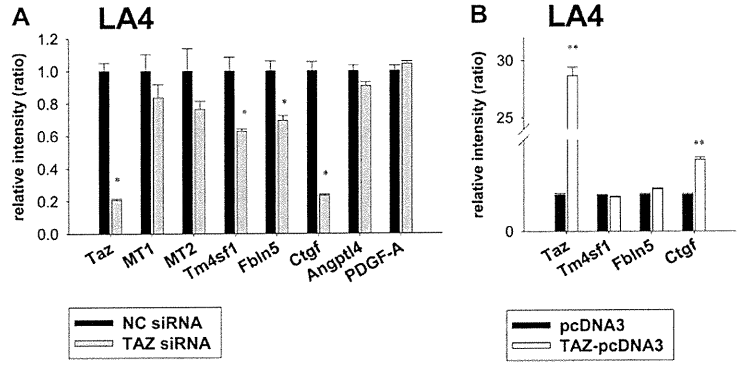

Figure 5. Quantitative real-time reverse transcription-polymerase chain reaction (RT-PCR) of LA4 cells (n = 4). (*A*) Relative expression levels of the indicated transcripts in control (NC) and *Taz* siRNA–treated LA4 cells. (*B*) Relative expression levels in control (pcDNA3) and *Taz*-overexpressing (TAZ-pcDNA3) LA4 cells. *See* text for definition of gene abbreviations. Data represent means ± SEM. $*P < 0.05$, $**P < 0.01$.

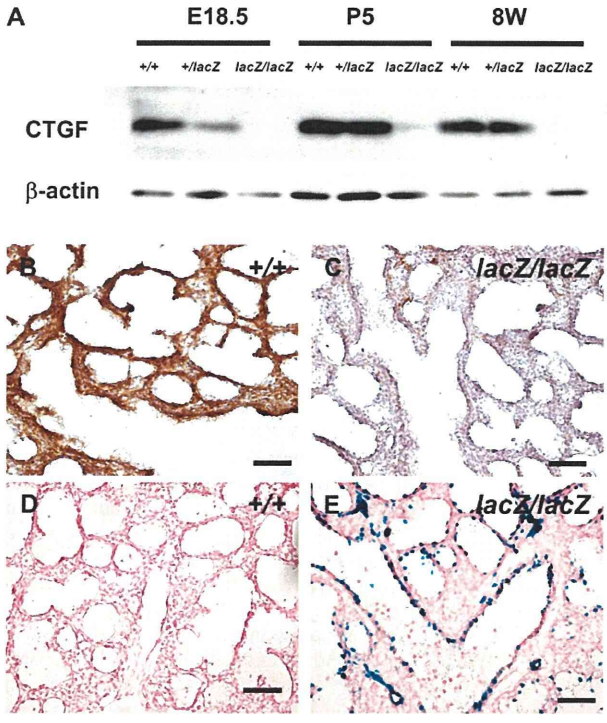

Figure 6. Decreased expression of connective tissue growth factor (CTGF) in *Taz*-deficient lungs. (*A*) Lysates from mouse lung tissues of wild-type, $Taz^{+/lacZ}$, and $Taz^{lacZ/LacZ}$ mice were blotted with anti-CTGF antibody and anti–β-actin antibodies. Shown are representative results of five experiments with similar results. (*B* and *C*) Staining of embryonic day 18.5 (E18.5) lungs with anti-CTGF antibody. (*D* and *E*) 5-Bromo-4-chloro-3-indolyl-β-D-galactopyranoside (X-Gal) staining of E18.5 lungs reflects transcriptional coactivator with PDZ-binding motif (TAZ) expression. *Scale bars*: 200 μm.

However, TGF-β stimulation and inhibition (using a small-molecule TGF-β receptor-1 kinase inhibitor, LY364947) considerably affected at least the expression of *PAI-1* mRNA in LA4 cells (Figure 7E), indicating that, in LA4 cells, TGF-β signal is important for the expression of *PAI-1*. The fact that there was no difference in *PAI-1* expression between *Taz*-knockout and wild-type lungs also suggests that total interruption of the TGF-β/smad cascade is less likely.

TAZ Can Control CTGF Expression in the Absence of TGF-β/smad Signals

Taz-deficient LA4 cells showed decreased expression of *Ctgf* and *PAI-1* (Figure 7D). We then investigated whether TGF-β inhibition blocks the regulation of *Ctgf* mRNA by TAZ. Interestingly, *Taz* overexpression without TGF-β stimulation up-regulated *Ctgf* mRNA (Figure 8A), but not *PAI-1* mRNA (Figure 8C). Furthermore, whereas *Taz* siRNA-treated LA4 cells expressed *PAI-1* mRNA in proportion to TGF-β concentration, although it was lower than the control (Figure 8D), *Taz* knockdown resulted in *Ctgf* mRNA expression reaching a plateau in spite of a high concentration of TGF-β (Figure 8B), implying that there exists another mechanism in the regulation of *Ctgf* expression by TAZ.

Dual-Luciferase Reporter Assay

We next investigated the interaction between the *Ctgf* promoter lesion and TAZ. The *Ctgf* promoter region contains a smad-binding site and TGF-β response element (28, 34). We cloned various lengths of DNA fragments of the *Ctgf* promoter region into pGL3 vectors (which are promoterless and enhancerless) (Figure 9A). As expected, CTGF(−122)-Luc showed no response to TGF-β stimulation because it contains neither a smad-binding site nor a TGF-β response element (Figure 9C), but it was affected by *Taz* overexpression as much as longer promoter regions (Figure 9B). The pLuc vector (containing a TATA box) with *Ctgf* promoter region at positions −123 to −76 also fully responded to *Taz* overexpression (Figure 9D). The sequence of this region, defined as the TAZ response element, was highly conserved between *Mus musculus* and *Homo sapiens* (Figure 9E). Thus, we concluded that the *Ctgf* promoter region contains a TAZ-responsive element and that TAZ can control *Ctgf* expression regardless of TGF-β signals.

Taz-heterozygous Mice Are Resistant to Bleomycin-induced Lung Fibrosis

TGF-β_1 is a key cytokine involved in the process of pulmonary fibrogenesis (35), and CTGF and PAI-1 regulated by TGF-β_1/smad signals also play important roles in the development of lung fibrotic diseases (11, 12, 36). Because this study showed that *Taz*-knockdown LA4 cells expressed lesser amounts of *Ctgf* and *PAI-1* mRNAs after TGF-β stimulation (Figures 8B and 8D) and that TAZ also controlled *Ctgf* expression in a TGF-β–independent pathway, we speculated that TAZ might be involved in the pathogenesis of lung fibrosis.

Although the *Taz* mRNA expression level in *Taz*-heterozygous mice was less than that in wild-type littermates (Figure 4B), the former developed normally and showed no obvious differences from wild-type mice at least until 15 months of age (*see* Figure E3 in the online supplement).

In the next set of experiments, we intraperitoneally injected *Taz*-heterozygous mice with bleomycin (10 mg/kg/d for 10 d). Such treatment resulted in a reduction of body weight of approximately 20% on Day 14 after starting the treatment. All mice returned to predosing body weight on about Day 21. The control, saline-treated mice exhibited no adverse effects and no weight loss throughout the 38 days of study. Histologically, bleomycin-treated wild-type mice showed focal areas of fibrosis with disruption of the alveolar architecture (Figure 10C). On the other hand, bleomycin-treated $Taz^{+/lacZ}$ mice had faint alveolitis and almost no fibrosis (Figure 10D). For semiquantitative analysis of lung fibrosis, we used the Ashcroft score. Criteria for grading lung fibrosis include fibrous thickening of alveolar walls, damage to lung architecture, and formation of fibrous bands or masses. Bleomycin-treated $Taz^{+/lacZ}$ mice showed a significantly low Ashcroft score compared with bleomycin-treated wild-type littermates (0.533 ± 0.098 vs. 1.013 ± 0.178; $P < 0.05$; Figure 10E).

The amount of hydroxyproline, which reflects the amount of collagen, was also reduced significantly in bleomycin-treated *Taz*-heterozygous mice compared with wild-type littermates (139.6 ± 2.7 vs. 166.7 ± 4.2; $P < 0.01$; Figure 10F). Needless to say, comparison of bleomycin and saline groups showed a significantly high amount in the bleomycin group regardless of their genotype. Furthermore, lung function analysis showed that bleomycin administration significantly increased lung elastance in wild-type mice, but not in $Taz^{+/lacZ}$ mice, and the lung elastance in bleomycin-treated $Taz^{+/lacZ}$ mice was significantly lower than in bleomycin-treated wild-type littermates (10.39 ± 0.57 vs. 13.66 ± 0.87; $P < 0.01$; Figure 10G).

BALF analysis revealed no obvious differences between $Taz^{+/lacZ}$ and wild-type mice (*see* Figure E4 in the online supplement), although bleomycin stimulation increased the cell count in BALF of both phenotypes. This result suggests that the

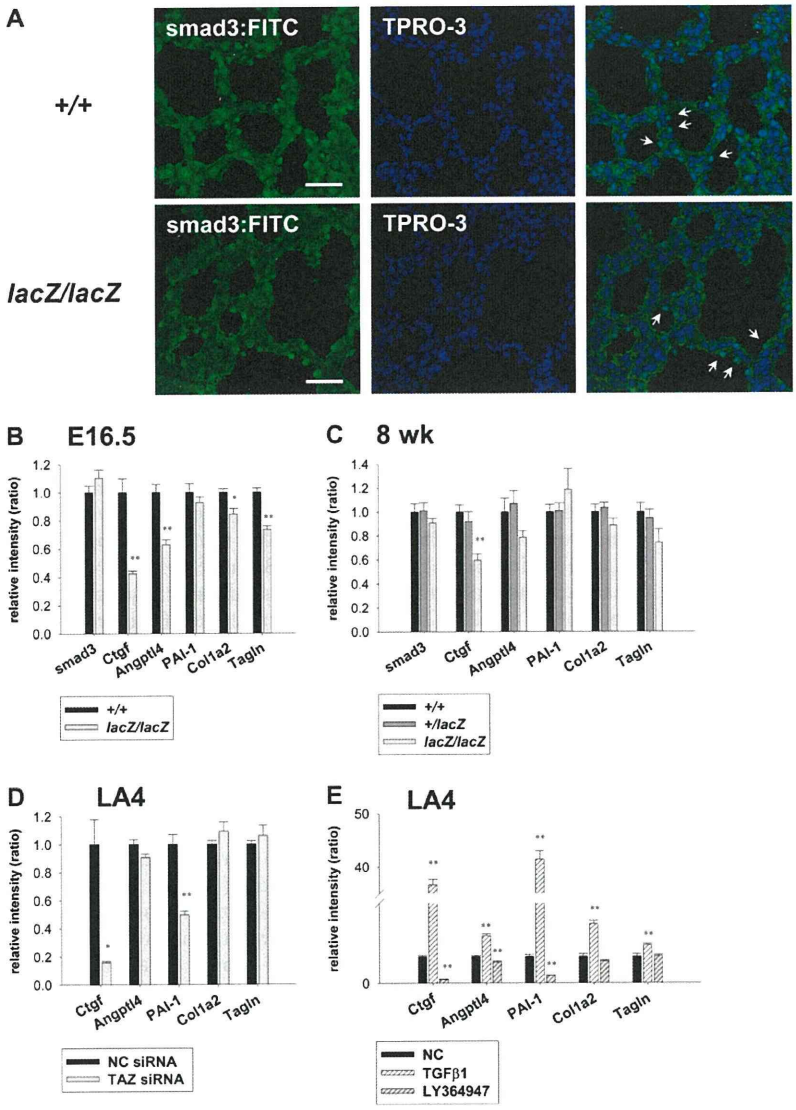

Figure 7. Expression of transforming growth factor (TGF)-β/smad-regulated genes. (*A*) Immunostaining of embryonic day 18.5 (E18.5) lungs with anti-Smad3 antibody shows expression of Smad3 in the nucleoli of epithelial cells in both wild-type and homozygous lungs (*arrows*). *Scale bars*: 100 μm. (*B* and *C*) Quantitative real-time reverse transcription-polymerase chain reaction (RT-PCR) of (*B*) E16.5 $Taz^{lacZ/LacZ}$ lungs versus their wild-type siblings and of (*C*) 8-week-old wild-type versus $Taz^{+/lacZ}$ versus $Taz^{lacZ/LacZ}$ mice. (*D* and *E*) Relative expression levels in *Taz* knockdown LA4 cells (n = 4) and in LA4 cells (n = 4) after TGF-β_1 stimulation (5 ng/ml, 24 h) or inhibition with LY364947 (10 μM, 24 h). NC = control. Data represent means ± SEM. $^*P < 0.05$, $^{**}P < 0.01$.

mild fibrosis in *Taz*-heterozygous mice might be explained by the difference in fibrogenic events rather than inflammation.

DISCUSSION

Adult *Taz*-deficient Mice Have Emphysema-like Lungs Because of Abnormal Distal Lung Morphogenesis

Our findings indicate that the lungs of adult *Taz*-deficient mice have emphysema-like features including enlarged air space and low elastance. The physiological data of *Taz*-deficient mice were so extraordinary that we could not measure them with the FlexiVent system. Therefore we analyzed them by the method described in METHODS.

These mice also exhibit abundant inflammatory cells in BALF, evidence of chronic inflammation in lungs, and some *Taz*-knockout lungs had small focal areas with inflammatory changes. There were some possible reasons for increased inflammation in *Taz*-deficient mice. One is the possibility that morphological and physiological abnormalities of *Taz*-deficient lungs caused susceptibility to infection or other kinds of inflammation, as often seen in human patients with chronic lung diseases. Another possibility is that decreased TGF-β/smad signals in *Taz*-deficient lung epithelial cells affected the production of proinflammatory cytokines such as tumor necrosis factor-α. However, the relationship between TAZ and inflammation is still unrevealed.

Sequential analysis of *Taz*-deficient lungs revealed abnormalities in distal lung morphogenesis, which resulted in an emphysema-like phenotype in the adult mouse. These results indicate that TAZ plays an important role in lung development, especially during the saccular and alveolar stages.

Possible Function of TAZ in Lung Development

Entry into the saccular stage is crucial for extrauterine survival. In this stage, widening of the peripheral air spaces distal to the terminal bronchioles allows for sufficient gas exchange. The lung parenchyma increases in size by branching of the terminal generations of the airway tree. Furthermore, during this period, preparation for real alveolarization starts by deposition of elastic fibers at the regions of future secondary septa (37). Epithelial cells differentiate into their descendants, including type 2 cells, under the influence of TTF-1, which is also essential for the complete induction of embryonic lung branching morphogenesis (17, 38). In this regard, a previous *in vitro* study

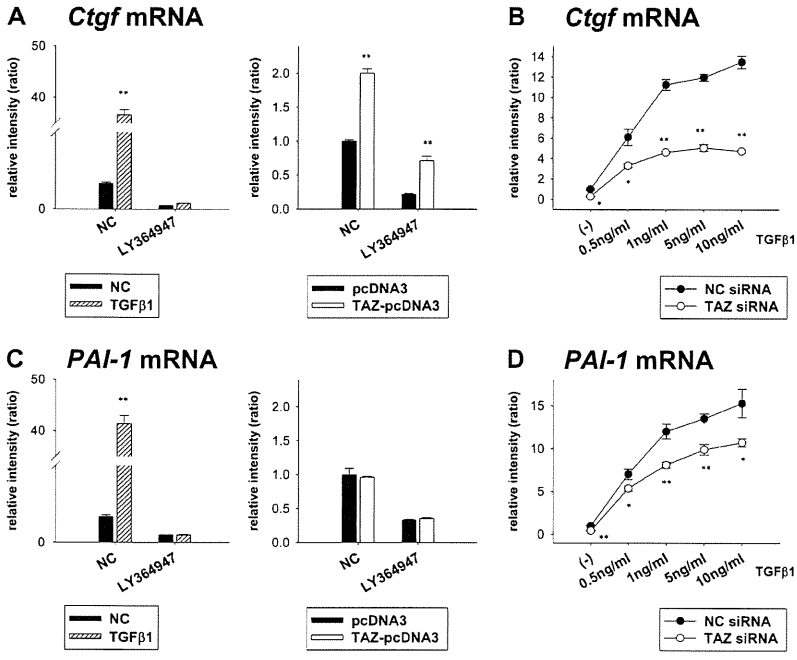

Figure 8. Comparison of expression levels of *Ctgf* and *PAI-1* (n = 4). (*A* and *C*) Expression levels of (*A*) *Ctgf* and (*C*) *PAI-1* in LA4 cells after transforming growth factor (TGF)-β stimulation (5 ng/ml, 24 h) or *Taz* overexpression with or without LY364947 (10 μM, 24 h). NC = control. (*B* and *D*) The response to TGF-β signals (0.5–10 ng/ml, 12 h) of *Taz* knockdown and nontreated LA4 cells. Data represent means ± SEM. $*P < 0.05$, $**P < 0.01$.

reported that TAZ serves as a coactivator of TTF-1 (3), but the expression levels of target genes of TTF-1 were not decreased in *Taz*-deficient mice. It is quite likely that, as far as TTF-1 transcription activity is concerned, TAZ deficiency can be compensated by alternative factors.

In the alveolar stage, newly formed walls, named secondary septa, subdivide the saccules incompletely into smaller units, the alveoli. The secondary septa demonstrate a doubled capillary layer separated by a sheet of connective tissue. This immature structure does not yet correspond to the thin interalveolar septa, in which a capillary monolayer occupies almost the whole space of the septum, and it undergoes more restructuring, called microvascular maturation (39). Because *Taz*-deficient mice showed decreased alveolarization in the alveolar stage, TAZ may be involved in the transcriptional regulation of factors participating in the formation of secondary septa.

Adult *Taz*-deficient mice also showed decreased expression of an endothelial cell marker gene (*Flk1*). Insufficient vascular development itself could cause abnormal lung development (40). However, it is difficult to show whether TAZ deficiency directly caused abnormality of vascular development leading to abnormal alveolarization, or, the other way around, decreased alveolar development was the main cause of insufficient vascular development.

In any case, TAZ deficiency seemed to affect development of secondary alveolar septa and distal vascular system, although TAZ existed at lung epithelial cells.

Gene Chip Experiment Revealed Some Candidate Genes Involved in Pathogenesis

Microarray analysis provided valuable information about possible underlying mechanism of the phenotype, although this was not fully examined. Among the genes whose expression was decreased in *Taz*-deficient lungs, Fbln5 and CTGF are important for the formation of extracellular matrix, and down-regulation may explain the lung phenotype of *Taz*-deficient mice. Furthermore, *Taz* knockdown by siRNA reduced the expression of *Ctgf* in LA4 cells, and *Taz* overexpression by expression vectors increased *Ctgf* expression, suggesting it has a close relationship with TAZ. Western blot and immunohistochemistry also revealed decreased CTGF protein expression in *Taz*-deficient lungs.

No angiogenic factors belonged to the list of down-regulated genes. We found that the expression of *PDGF-A* mRNA was decreased to some degree by real-time RT-PCR. But *in vitro* studies could not reveal the relationship between TAZ and PDGF-A.

CTGF contains several domains that mediate interactions with growth factors, integrins, and extracellular matrix components. CTGF is considered to play a role in extracellular matrix production, based on its ability to mediate collagen deposition during wound healing. CTGF is also a major inducer of extracellular matrix production in fibrotic diseases, including lung fibrosis (11, 41). Analysis of *Ctgf*-deficient mice revealed that CTGF is important for chondrogenesis and angiogenesis during skeletal development (42) and lung development (24). Because the hypoplastic lungs of *Ctgf*-deficient mice were induced partly by restricted thoracic expansion, the role of CTGF in lung development in the strict sense of the word had not been fully examined. Although conditional knockout mice would be useful to clarify its role, we thought that CTGF could affect mesenchymal cells and vascular development in the lung.

Another problem concerns why the abnormality of *Taz*-deficient lungs appeared only in the parenchymal area, because TAZ and CTGF were expressed in both airway epithelia and lung parenchyma. One possibility is that because TAZ deficiency has almost no influence on epithelial cells, airway epithelial cells, which are not so dependent on mesenchyme as alveolar cells, could develop normally. *Ctgf* conditional knockout mice might also clear up this point.

Considered together, we concluded that CTGF is a potentially key molecule responsible for the abnormal distal lung development in *Taz*-deficient mice.

TAZ Controls CTGF Expression in a TGF-β–independent Way

CTGF expression is up-regulated by various signals, such as TGF-β/smad (28), dexamethasone (43), α-tocopherol (44), and me-

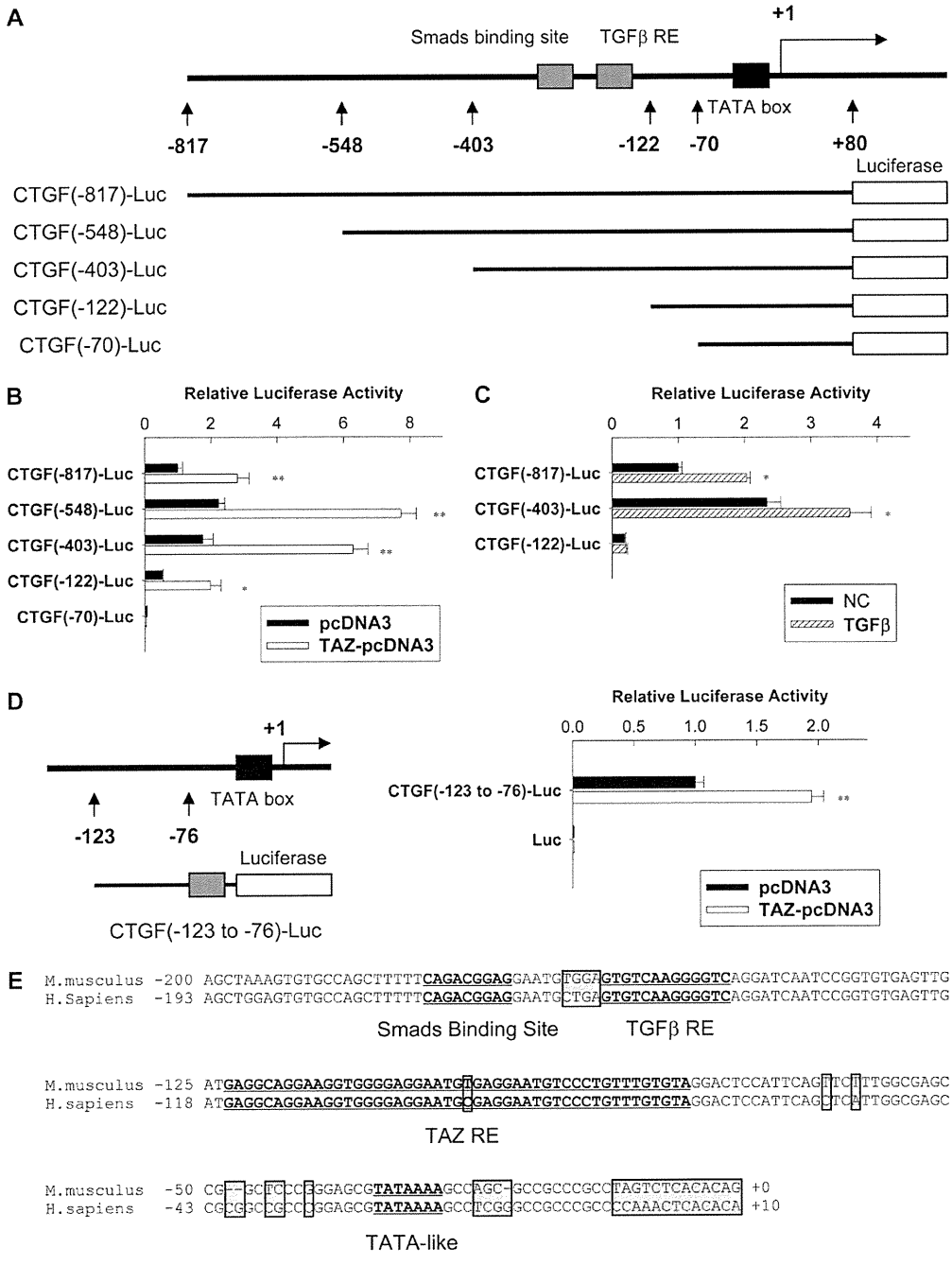

Figure 9. Dual-luciferase reporter assay (n = 4–6). (*A*) Schematic representation of the *Ctgf* promoter region. RE = response element. (*B* and *C*) Luciferase activity of various lengths of the *Ctgf* promoter region in pGL3 vector with *Taz* overexpression or transforming growth factor (TGF)-β stimulation (5 ng/ml, 24 h). NC = control. (*D*) Luciferase activity of transcriptional coactivator with PDZ-binding motif (TAZ) response element (−123 to −76) in pLuc. Data represent means ± SEM. $^{*}P < 0.05$, $^{**}P < 0.01$. (*E*) Comparison of the sequences of the *Ctgf* promoter region between *Mus musculus* and *Homo sapiens*. Sequences in the *shaded boxes* are not identical.

chanical stress (45). Among them, TGF-β/smad signals have been well studied. TGF-β receptors directly phosphorylate smad2/3, and the phosphorylated smad2/3 forms complexes with smad4. In the nucleus, smads regulate the transcription of *Ctgf* by interacting with the TGF-β response element within the *Ctgf* promoter region (28). It has been reported that TAZ, as a binding partner of smads, is crucial for the nuclear accumulation of smads in embryonic stem cells (5). On the basis of these findings, we speculate that insufficient nuclear accumulation of smads in *Taz*-deficient mice might explain the lung phenotype.

However, immunohistochemistry showed nucleolar smad3 in *Taz*-deficient lung epithelial cells, whereas the number of these cells was slightly smaller than that in wild-type lung. Quantitative RT-PCR showed that the expression of other target genes of smads were not affected to the same extent. It is true that TAZ deficiency reduced the effects of TGF-β/smad signals, but insufficient TGF-β/smad signals cannot fully explain the decreased expression of CTGF and the lung phenotype of *Taz*-deficient mice.

The *in vitro* study revealed that TAZ increased the expression of *Ctgf* mRNA without TGF-β stimulation and interacted with a more proximal region than the TGF-β response element, defined as the TAZ response element, in the *Ctgf* promoter sequence. The TAZ response element is composed of DNA sequence at bp −123 to −76 in the *Ctgf* promoter region. It contains a putative NF-κB–binding site at bp −97 to −87 (AGGAATGTCCC), but its relationship with TAZ or *Ctgf* expression remains obscure.

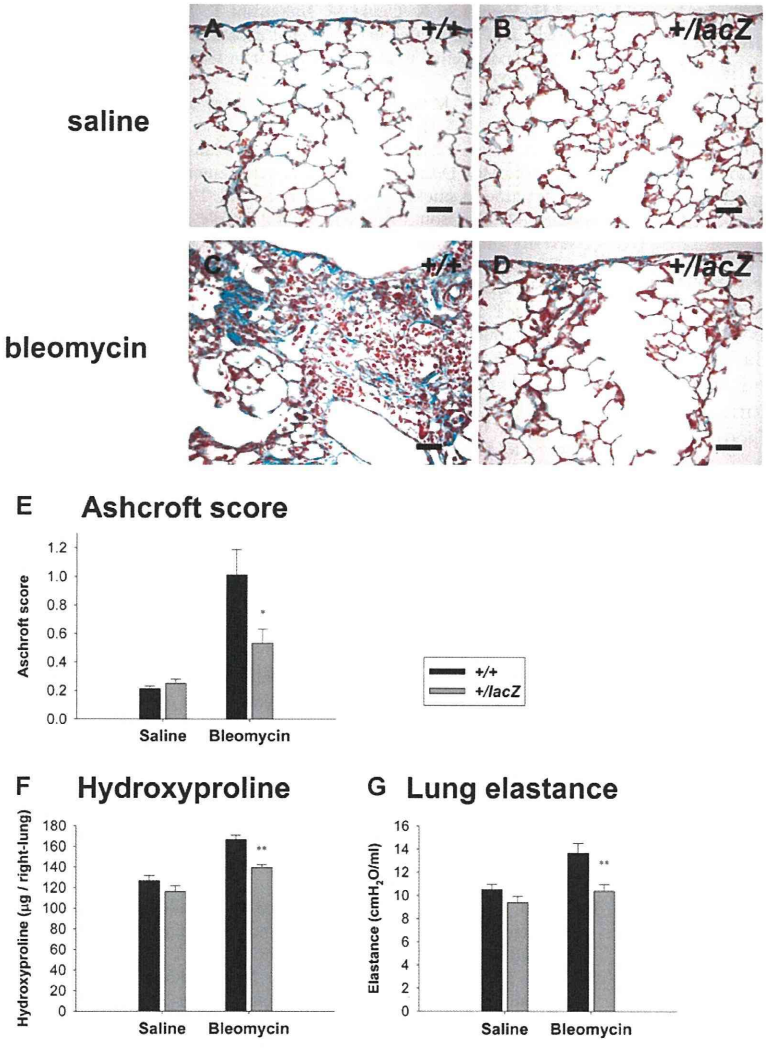

Figure 10. Bleomycin-induced lung fibrosis in *Taz*$^{+/lacZ}$ mice and wild-type mice (n = 6). Control mice received saline injections. (*A–D*) Masson trichrome staining of the lung sections. *Scale bars*: 50 μm. (*E*) Ashcroft score. (*F*) Amount of hydroxyproline in whole right lung. (*G*) Lung elastance. Data represent means ± SEM. *$P < 0.05$, **$P < 0.01$.

Involvement of TAZ in Pathogenesis of Bleomycin-induced Lung Fibrosis

Taz-heterozygous mice expressed reduced *Taz* mRNA expression, but showed no obvious abnormality. However, they were more resistant to bleomycin-induced lung fibrosis, thus indicating that TAZ plays a significant role in lung fibrosis. In analyzing these data, the strain of mice is crucially important. The mice in this experiment, however, had been backcrossed to the C57BL6/J strain for more than nine generations, and our preliminary data showed that *Taz* wild-type mice and C57BL6/J mice had almost the same response to bleomycin in terms of Ashcroft score, the amount of hydroxyproline, and lung elastance.

As stated previously, TAZ can reinforce the TGF-β/smad signals and increase *Ctgf* expression, which in turn is involved in pulmonary fibrogenesis. Therefore, we suggest that reduced TGF-β/smad signals and *Ctgf* expression in *Taz*$^{+/lacZ}$ mice could be responsible for the tolerance to bleomycin-induced fibrogenesis.

Clinical Implications

Taz-deficient adult mice showed an emphysema-like phenotype due to abnormal distal lung development. These mice can provide useful information for our understanding of the pathogenesis of emphysema. Because it is widely accepted that human emphysema is caused by the disruption of fully developed alveoli, it should be noted that spontaneously developed emphysema caused by developmental abnormalities in many gene-targeted animal models including *Taz*-deficient mice does not represent the same pathological state as human emphysema. However, developmental risk factors could underlie at least some susceptibility to apparently adult-onset chronic lung disease, including emphysema. For example, failure in correct matrix organization may predispose to certain serious degenerative diseases such as emphysema (46). Another possibility is that dysplastic or degraded matrix can provide neither the structural niche nor environmental cues for alveolar stem/progenitor cells to assume the correct phenotype and/or repair the correct alveolar cell lineage (47, 48). Therefore, the function of TAZ in lung development may be directly associated with the pathogenesis of emphysema. Taken together, we conclude that the *Taz*-deficient mouse is a novel model of pulmonary emphysema. The present study may provide a few clues to the genetic susceptibility to chronic obstructive pulmonary disease.

The fact that the heterozygous mice are resistant to bleomycin-induced fibrosis also could be important from the clinical point of view. Bleomycin is an important, clinically relevant antineoplastic agent used as first-line therapy in the management of

many human cancers, including Hodgkin's disease, germ cell tumors, and others. However, bleomycin induces pulmonary fibrosis in a dose-dependent manner, and fibrosis is a major dose-limiting side effect. Bleomycin-induced lung fibrosis is also thought to be a mouse model of human interstitial pneumonias (49). One form, idiopathic pulmonary pneumonia (IPF), is characterized by fibroblast proliferation and extracellular matrix remodeling, which result in irreversible distortion of the lung architecture. IPF is a progressive and usually fatal condition with no available cure (50). The use of bleomycin in mouse models threw light on a number of signaling pathways associated with IPF, although the translation from successful experimental models to effective clinical therapy has not proved to be easy. This study presents TAZ as a new and important factor in the pathogenesis of bleomycin-induced lung fibrosis and probably IPF. Because *Taz*-heterozygous mice develop normally, TAZ might have a close relationship with a genetic factor of susceptibility to these diseases.

There is no published report about *Taz* mutants in human emphysema or IPF, and whether TAZ could be a target gene of these diseases awaits further investigation. However, the fact that TAZ deficiency is not lethal and homozygous mice have the abnormality apparently only in kidneys and lungs also makes us expect that TAZ is a potentially suitable target for the design of new therapies.

Conflict of Interest Statement: None of the authors has a financial relationship with a commercial entity that has an interest in the subject of this manuscript.

References

1. Kanai F, Marignani PA, Sarbassova D, Yagi R, Hall RA, Donowitz M, Hisaminato A, Fujiwara T, Ito Y, Cantley LC, *et al.* Taz: a novel transcriptional co-activator regulated by interactions with 14-3-3 and PDZ domain proteins. *EMBO J* 2000;19:6778–6791.
2. Hong JH, Hwang ES, McManus MT, Amsterdam A, Tian Y, Kalmukova R, Mueller E, Benjamin T, Spiegelman BM, Sharp PA, *et al.* Taz, a transcriptional modulator of mesenchymal stem cell differentiation. *Science* 2005;309:1074–1078.
3. Park KS, Whitsett JA, Di Palma T, Hong JH, Yaffe MB, Zannini M. TAZ interacts with TTF-1 and regulates expression of surfactant protein-C. *J Biol Chem* 2004;279:17384–17390.
4. Murakami M, Tominaga J, Makita R, Uchijima Y, Kurihara Y, Nakagawa O, Asano T, Kurihara H. Transcriptional activity of Pax3 is co-activated by TAZ. *Biochem Biophys Res Commun* 2006; 339:533–539.
5. Varelas X, Sakuma R, Samavarchi-Tehrani P, Peerani R, Rao BM, Dembowy J, Yaffe MB, Zandstra PW, Wrana JL. TAZ controls Smad nucleocytoplasmic shuttling and regulates human embryonic stem-cell self-renewal. *Nat Cell Biol* 2008;10:837–848.
6. Hong JH, Yaffe MB. TAZ: a β-catenin–like molecule that regulates mesenchymal stem cell differentiation. *Cell Cycle* 2006;5:176–179.
7. Makita R, Uchijima Y, Nishiyama K, Amano T, Chen Q, Takeuchi T, Mitani A, Nagase T, Yatomi Y, Aburatani H, *et al.* Multiple renal cysts, urinary concentration defects, and pulmonary emphysematous changes in mice lacking TAZ. *Am J Physiol Renal Physiol* 2008;294: F542–F553.
8. Tian Y, Kolb R, Hong JH, Carroll J, Li D, You J, Bronson R, Yaffe MB, Zhou J, Benjamin T. TAZ promotes PC2 degradation through a $SCF^{\beta\text{-}Trcp}$ E3 ligase complex. *Mol Cell Biol* 2007;27:6383–6395.
9. Hossain Z, Ali SM, Ko HL, Xu J, Ng CP, Guo K, Qi Z, Ponniah S, Hong W, Hunziker W. Glomerulocystic kidney disease in mice with a targeted inactivation of *Wwtr1*. *Proc Natl Acad Sci USA* 2007;104: 1631–1636.
10. Kasai H, Allen JT, Mason RM, Kamimura T, Zhang Z. TGF-β_1 induces human alveolar epithelial to mesenchymal cell transition (EMT). *Respir Res* 2005;6:56–70.
11. Lasky JA, Ortiz LA, Tonthat B, Hoyle GW, Corti M, Athas G, Lungarella G, Brody A, Friedman M. Connective tissue growth factor mRNA expression is upregulated in bleomycin-induced lung fibrosis. *Am J Physiol* 1998;275:L365–L371.
12. Pan LH, Yamauchi K, Uzuki M, Nakanishi T, Takigawa M, Inoue H, Sawai T. Type II alveolar epithelial cells and interstitial fibroblasts express connective tissue growth factor in IPF. *Eur Respir J* 2001;17: 1220–1227.
13. Thurlbeck WM. Measurement of pulmonary emphysema. *Am Rev Respir Dis* 1967;95:752–764.
14. Saetta M, Shiner RJ, Angus GE, Kim WD, Wang NS, King M, Ghezzo H, Cosio MG. Destructive index: a measurement of lung parenchymal destruction in smokers. *Am Rev Respir Dis* 1985;131:764–769.
15. Ashcroft T, Simpson JM, Timbrell V. Simple method of estimating severity of pulmonary fibrosis on a numerical scale. *J Clin Pathol* 1988;41:467–470.
16. Nagase T, Uozumi N, Ishii S, Kita Y, Yamamoto H, Ohga E, Ouchi Y, Shimizu T. A pivotal role of cytosolic phospholipase A_2 in bleomycin-induced pulmonary fibrosis. *Nat Med* 2002;8:480–484.
17. Minoo P, Su G, Drum H, Bringas P, Kimura S. Defects in tracheoesophageal and lung morphogenesis in *Nkx2.1*$^{-/-}$ mouse embryos. *Dev Biol* 1999;209:60–71.
18. Bostrom H, Willetts K, Pekny M, Leveen P, Lindahl P, Hedstrand H, Pekna M, Hellstrom M, Gebre-Medhin S, Schalling M, *et al.* PDGF-A signaling is a critical event in lung alveolar myofibroblast development and alveogenesis. *Cell* 1996;85:863–873.
19. Thirumoorthy N, Manisenthil Kumar KT, Shyam Sundar A, Panayappan L, Chatterjee M. Metallothionein: an overview. *World J Gastroenterol* 2007;13:993–996.
20. Kao YR, Shih JY, Wen WC, Ko YP, Chen BM, Chan YL, Chu YW, Yang PC, Wu CW, Roffler SR. Tumor-associated antigen 16 and the invasion of human lung cancer cells. *Clin Cancer Res* 2003;9:2807–2816.
21. Nakamura T, Lozano PR, Ikeda Y, Iwanaga Y, Hinek A, Minamisawa S, Cheng CF, Kobuke K, Dalton N, Takada Y, *et al.* Fibulin-5/dance is essential for elastogenesis *in vivo*. *Nature* 2002;415:171–175.
22. Luft FC. CCN2, the connective tissue growth factor. *J Mol Med* 2008; 861:1–3.
23. Grotendorst GR. Connective tissue growth factor: a mediator of TGF-β action on fibroblasts. *Cytokine Growth Factor Rev* 1997;8:171–179.
24. Baguma-Nibasheka M, Kablar B. Pulmonary hypoplasia in the connective tissue growth factor (CTGF) null mouse. *Dev Dyn* 2008;237:485–493.
25. Padua D, Zhang XH, Wang Q, Nadal C, Gerald WL, Gomis RR, Massague J. TGFβ primes breast tumors for lung metastasis seeding through angiopoietin-like 4. *Cell* 2008;133:66–77.
26. Schittny JC, Mund SI, Stampanoni M. Evidence and structural mechanism for late lung alveolarization. *Am J Physiol* 2008;294: L246–L254.
27. Wu S, Peng J, Duncan MR, Kasisomayajula K, Grotendorst G, Bancalari E. ALK-5 mediates endogenous and TGF-β_1-induced expression of connective tissue growth factor in embryonic lung. *Am J Respir Cell Mol Biol* 2007;36:552–561.
28. Holmes A, Abraham DJ, Sa S, Shiwen X, Black CM, Leask A. CTGF and SMADs, maintenance of scleroderma phenotype is independent of SMAD signaling. *J Biol Chem* 2001;276:10594–10601.
29. Bonniaud P, Kolb M, Galt T, Robertson J, Robbins C, Stampfli M, Lavery C, Margetts PJ, Roberts AB, Gauldie J. Smad3 null mice develop airspace enlargement and are resistant to TGF-β-mediated pulmonary fibrosis. *J Immunol* 2004;173:2099–2108.
30. Chen H, Sun J, Buckley S, Chen C, Warburton D, Wang XF, Shi W. Abnormal mouse lung alveolarization caused by Smad3 deficiency is a developmental antecedent of centrilobular emphysema. *Am J Physiol* 2005;288:L683–L691.
31. Gauldie J, Kolb M, Ask K, Martin G, Bonniaud P, Warburton D. Smad3 signaling involved in pulmonary fibrosis and emphysema. *Proc Am Thorac Soc* 2006;3:696–702.
32. Inagaki Y, Nemoto T, Nakao A, Dijke P, Kobayashi K, Takehara K, Greenwel P. Interaction between GC box binding factors and Smad proteins modulates cell lineage-specific α2(I) collagen gene transcription. *J Biol Chem* 2001;276:16573–16579.
33. Yu H, Konigshoff M, Jayachandran A, Handley D, Seeger W, Kaminski N, Eickelberg O. Transgelin is a direct target of TGF-β/Smad3-dependent epithelial cell migration in lung fibrosis. *FASEB J* 2008;22: 1778–1789.
34. Grotendorst GR, Okochi H, Hayashi N. A novel transforming growth factor β response element controls the expression of the connective tissue growth factor gene. *Cell Growth Differ* 1996;7:469–480.
35. Gauldie J, Kolb M, Sime PJ. A new direction in the pathogenesis of idiopathic pulmonary fibrosis? *Respir Res* 2002;3:1.

36. Liu RM. Oxidative stress, plasminogen activator inhibitor 1, and lung fibrosis. *Antioxid Redox Signal* 2008;10:303–319.
37. Wasowicz M, Yokoyama S, Kashima K, Nakayama I. The connective tissue compartment in the terminal region of the developing rat lung: an ultrastructural study. *Acta Anat (Basel)* 1996;156:268–282.
38. Minoo P, Hamdan H, Bu D, Warburton D, Stepanik P, deLemos R. TTF-1 regulates lung epithelial morphogenesis. *Dev Biol* 1995;172: 694–698.
39. Burri PH. Structural aspects of postnatal lung development: alveolar formation and growth. *Biol Neonate* 2006;89:313–322.
40. Warburton D, Schwarz M, Tefft D, Flores-Delgado G, Anderson KD, Cardoso WV. The molecular basis of lung morphogenesis. *Mech Dev* 2000;92:55–81.
41. Chen CM, Wang LF, Chou HC, Lang YD, Lai YP. Up-regulation of connective tissue growth factor in hyperoxia-induced lung fibrosis. *Pediatr Res* 2007;62:128–133.
42. Ivkovic S, Yoon BS, Popoff SN, Safadi FF, Libuda DE, Stephenson RC, Daluiski A, Lyons KM. Connective tissue growth factor coordinates chondrogenesis and angiogenesis during skeletal development. *Development* 2003;130:2779–2791.
43. Okada H, Kikuta T, Inoue T, Kanno Y, Ban S, Sugaya T, Takigawa M, Suzuki H. Dexamethasone induces connective tissue growth factor expression in renal tubular epithelial cells in a mouse strain–specific manner. *Am J Pathol* 2006;168:737–747.
44. Villacorta L, Graca-Souza AV, Ricciarelli R, Zingg JM, Azzi A. α-Tocopherol induces expression of connective tissue growth factor and antagonizes tumor necrosis factor-α–mediated downregulation in human smooth muscle cells. *Circ Res* 2003;92:104–110.
45. Chaqour B, Goppelt-Struebe M. Mechanical regulation of the Cyr61/CCN1 and CTGF/CCN2 proteins. *FEBS J* 2006;273:3639–3649.
46. Warburton D, Gauldie J, Bellusci S, Shi W. Lung development and susceptibility to chronic obstructive pulmonary disease. *Proc Am Thorac Soc* 2006;3:668–672.
47. Warburton D, Berberich MA, Driscoll B. Stem/progenitor cells in lung morphogenesis, repair, and regeneration. *Curr Top Dev Biol* 2004;64: 1–16.
48. Weiss DJ, Berberich MA, Borok Z, Gail DB, Kolls JK, Penland C, Prockop DJ. Adult stem cells, lung biology, and lung disease. NHLBI/Cystic Fibrosis Foundation workshop. *Proc Am Thorac Soc* 2006;3:193–207.
49. Chua F, Gauldie J, Laurent GJ. Pulmonary fibrosis: searching for model answers. *Am J Respir Cell Mol Biol* 2005;33:9–13.
50. Swigris JJ, Kuschner WG, Kelsey JL, Gould MK. Idiopathic pulmonary fibrosis: challenges and opportunities for the clinician and investigator. *Chest* 2005;127:275–283.

Developmental Cell
Article

The Hippo Signaling Pathway Components Lats and Yap Pattern Tead4 Activity to Distinguish Mouse Trophectoderm from Inner Cell Mass

Noriyuki Nishioka,[1] Ken-ichi Inoue,[2] Kenjiro Adachi,[3] Hiroshi Kiyonari,[2] Mitsunori Ota,[1] Amy Ralston,[4] Norikazu Yabuta,[5] Shino Hirahara,[1] Robert O. Stephenson,[4] Narumi Ogonuki,[6] Ryosuke Makita,[7] Hiroki Kurihara,[7] Elizabeth M. Morin-Kensicki,[8] Hiroshi Nojima,[5] Janet Rossant,[4] Kazuki Nakao,[2] Hitoshi Niwa,[3] and Hiroshi Sasaki[1,*]
[1]Laboratory for Embryonic Induction
[2]Laboratory for Animal Resources and Genetic Engineering
[3]Laboratory for Pluripotent Stem Cells
RIKEN Center for Developmental Biology, 2-2-3 Minatojima-minamimachi, Chuo-ku, Kobe, Hyogo 650-0047, Japan
[4]Program in Developmental and Stem Cell Biology, Hospital for Sick Children Research Institute, MARS Building, Toronto Medical Discovery Tower, 101 College Street, Toronto, ON M5G 1L7, Canada
[5]Department of Molecular Genetics, Research Institute for Microbial Diseases, Osaka University, Yamadaoka 3-1, Suita, Osaka 565-0871, Japan
[6]RIKEN Bioresource Center, 3-1-1 Koyadai, Tsukuba, Ibaraki 305-0074, Japan
[7]Department of Physiological Chemistry and Metabolism, Graduate School of Medicine, The University of Tokyo, 7-3-1 Hongo, Bunkyo-ku, Tokyo 113-0033, Japan
[8]Department of Cell and Developmental Biology, University of North Carolina at Chapel Hill, Chapel Hill, NC 27599, USA
*Correspondence: sasaki@cdb.riken.jp
DOI 10.1016/j.devcel.2009.02.003

SUMMARY

Outside cells of the preimplantation mouse embryo form the trophectoderm (TE), a process requiring the transcription factor Tead4. Here, we show that transcriptionally active Tead4 can induce *Cdx2* and other trophoblast genes in parallel in embryonic stem cells. In embryos, the Tead4 coactivator protein Yap localizes to nuclei of outside cells, and modulation of Tead4 or Yap activity leads to changes in Cdx2 expression. In inside cells, Yap is phosphorylated and cytoplasmic, and this involves the Hippo signaling pathway component Lats. We propose that active Tead4 promotes TE development in outside cells, whereas Tead4 activity is suppressed in inside cells by cell contact- and Lats-mediated inhibition of nuclear Yap localization. Thus, differential signaling between inside and outside cell populations leads to changes in cell fate specification during TE formation.

INTRODUCTION

During mouse development, the first lineage specified is the trophoblast/placenta lineage, set aside during blastocyst formation. In the blastocyst, the trophoblast, or trophectoderm (TE), surrounds the inner cell mass (ICM), which will give rise to the fetus and other extraembryonic tissues. The homeodomain transcription factor Cdx2 is expressed in the TE at the blastocyst stage. Cdx2 is required for TE development and is sufficient to promote trophoblast fate in ICM-derived embryonic stem (ES) cells, including suppression of ICM and induction of TE genes (Niwa et al., 2005; Strumpf et al., 2005). Conversely, ICM fates are regulated by a distinct set of transcription factors, including the POU family transcription factor Oct3/4 (encoded by *Pou5f1*). Prior to blastocyst formation, Cdx2 and Oct3/4 are initially co-expressed throughout the embryo (Dietrich and Hiiragi, 2007; Palmieri et al., 1994; Ralston and Rossant, 2008). Mutual antagonism between these two factors may contribute to the eventual segregation of their expression domains (Niwa et al., 2005), with Cdx2 in outside cells of the TE and Oct3/4 in inside cells of the ICM. However, molecular mechanisms that initially interpret inside/outside positional information within the embryo to establish this pattern are not known.

We and others recently showed that the TEAD/TEF family transcription factor Tead4 is essential for TE development and Cdx2 expression prior to the blastocyst stage (Nishioka et al., 2008; Yagi et al., 2007). This provided the first clue about molecular mechanisms acting upstream of the TE/ICM lineage distinction. However, whether Tead4 acted permissively or instructively in this process was unclear, since Tead4 itself was not restricted to outside cells (Nishioka et al., 2008).

Here, we sought to identify cofactors and signaling components that could impart positional information to spatially regulate Tead4 activity in the embryo. Many lines of evidence have suggested that TEAD-mediated transcription is regulated by the Ser/Thr kinase Hippo in *Drosophila*, or Stk3 (Mst) in mice. In *Drosophila*, Hippo inhibits the Yorkie (Yki) coactivator and suppresses cell proliferation (Huang et al., 2005). These activities are mediated by a Tead protein, Scalloped (Goulev et al., 2008; Wu et al., 2008; Zhang et al., 2008b). In mammals, Hippo signaling comprises a growth-regulating pathway, which controls cell contact-mediated inhibition of proliferation (see reviews Pan, 2007; Reddy and Irvine, 2008; Saucedo and Edgar, 2007). In this context, cell-cell contact regulates nuclear accumulation of a Yki homolog, Yes-associated protein 1 (Yap1, Yap hereafter), through Hippo signaling and controls cell proliferation by regulating transcriptional activity of Tead proteins (Ota and Sasaki, 2008; Zhao et al., 2007, 2008). In the mouse embryo,

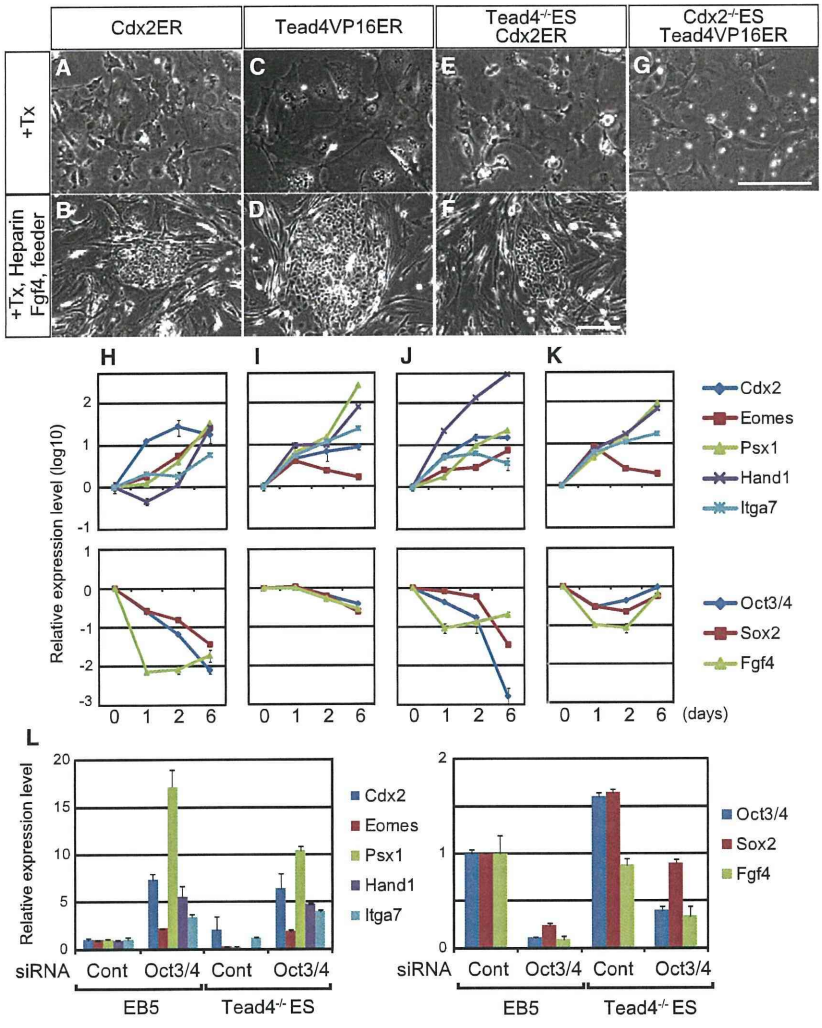

Figure 1. Tead4 Regulates Multiple Trophoblast Genes in ES Cells

(A–G) Morphologies of ES cells treated for 6 days with Tx in (A, C, E, and G) ES cell medium and in (B, D, and F) TS cell culture medium in the presence of feeder cells.

(H–K) Expression of trophoblast (upper panels) and ES/ICM (lower panels) genes in representative clones of (H) 5ECER4 (EB5 + Cdx2ER), (I) 5TVER7 (EB5 + Tead4VP16ER), (J) T4CER10 (*Tead4*$^{-/-}$ + Cdx2ER), and (K) CTVER5 (*Cdx2*$^{-/-}$ + Tead4VP16ER) cells after Tx treatment for the indicated time periods.

(L) Expression of trophoblast (left panel) and ES/ICM (right panel) genes in EB5 (control) and *Tead4*$^{-/-}$ ES cells after transfection of control or Oct3/4 siRNAs.

Tead1$^{-/-}$; *Tead2*$^{-/-}$ mutants die soon after implantation due to reduced cell proliferation and increased apoptosis (Sawada et al., 2008). *Tead1/2* interact genetically with *Yap* (Sawada et al., 2008), suggesting that the roles of these genes in Hippo signaling are conserved in mice.

We examined the role of Tead4 in TE development using both ES cells and preimplantation embryos. We show that active Tead4 can promote multiple trophoblast genes in parallel, including *Cdx2*. We next show that, in the embryo, the Tead coactivator Yap localizes to nuclei only in outside cells and is excluded from inside cell nuclei by the Hippo signaling pathway component Lats. These observations suggest that Tead4/Yap interpret positional information along the inside/outside axis of the embryo to restrict expression of Cdx2 and TE fates to outside cells.

RESULTS

Tead4 Instructively Regulates Multiple Trophoblast Genes in ES Cells

Although Tead4 is required for establishment of the TE lineage in the mouse embryo (Nishioka et al., 2008; Yagi et al., 2007), the sufficiency of Tead4 to promote TE fate has not been reported. We examined the ability of Tead4 to promote trophoblast differentiation in ES cells. For comparison, we used the ES cell line 5ECER4 (Niwa et al., 2005), which stably expresses a tamoxifen (Tx)-inducible fusion between Cdx2 and a modified ligand-binding domain of the estrogen receptor (ER) (Cdx2ER). Consistent with previous analyses (Niwa et al., 2005), treatment of 5ECER4 cells with Tx led to flattened morphologies reminiscent of trophoblast cells (Figure 1A), induction of trophoblast genes, and downregulation of ES cell genes (Figure 1H). Using trophoblast stem (TS) cell culture conditions (Tanaka et al., 1998), TS-like cells could be derived from this line (Figure 1B). These observations are consistent with previous analyses (Niwa et al., 2005) and provide a standard against which to evaluate Tead4 activity in ES cells.

We next examined the ability of Tead4 to induce trophoblast fate in ES cells. We established ES cell lines stably expressing a Tx-inducible form of active Tead4 (Tead4VP16ER), which consisted of the Tead4 DNA-binding domain fused to the transcriptional activation domain of herpes simplex virus VP16, followed by the ER domain. After treatment with Tx, multiple independent clones exhibited morphological changes similar to Cdx2 overexpression (Figure 1C). Treated Tead4VP16-expressing clones also expressed trophoblast genes (Figure 1I), and TS-like cells could be derived under TS cell culture conditions (Figure 1D). Thus, constitutively active Tead4 is sufficient to promote trophoblast fate in ES cells.

Cdx2 Is a Major Target of Tead4

Tead4 is genetically upstream of *Cdx2* during TE formation in the embryo (Nishioka et al., 2008; Yagi et al., 2007), suggesting that *Tead4* is not required for Cdx2-mediated trophoblast gene expression in ES cells. To test this hypothesis, we established feeder-free *Tead4*$^{-/-}$ ES cell lines (Nishioka et al., 2008) that stably express Cdx2ER, and we examined their ability to adopt

trophoblast fate. After treatment with Tx, multiple independent clones exhibited similar trophoblast-like morphologies (Figure 1E). In addition, trophoblast genes were upregulated, whereas ES genes were downregulated (Figure 1J), suggesting that *Tead4* is not required for Cdx2-mediated induction of trophoblast differentiation in ES cells. To examine the requirement for *Tead4* in long-term TS-like potential, we cultured these cells under TS conditions. Colonies with TS-like morphology could be derived, but could not be maintained as TS cells (Figure 1F and data not shown), indicating that *Cdx2* cannot fully substitute for *Tead4* in the trophoblast lineage.

As another means by which to examine the epistatic relationship between *Tead4* and *Cdx2*, we established *Cdx2*$^{-/-}$ ES cells (Niwa et al., 2005) stably expressing Tead4VP16ER, and we examined their ability to adopt trophoblast fate. After treatment with Tx, multiple independent clones also exhibited trophoblast-like morphology (Figure 1G) and trophoblast gene expression (Figure 1K). Tead4 can therefore regulate trophoblast gene expression independently of *Cdx2*. However, TS-like colonies could not be derived from these cells, suggesting that *Cdx2* is essential for proper trophoblast lineage development. Taken together, these observations suggest that Tead4 promotes trophoblast fate through both *Cdx2*-dependent and -independent pathways, and that Cdx2 is a major mediator of *Tead4*-dependent changes in trophoblast gene expression.

Tead4 Is Dispensable for *Cdx2* Expression when *Oct3/4* Levels Are Reduced

In ES cells, Oct3/4 suppresses *Cdx2*, and reduction of *Oct3/4* leads to upregulation of *Cdx2* expression and formation of TS-like cells (Niwa et al., 2000, 2005). Because *Tead4* is required for *Cdx2* expression and TE development in vivo (Nishioka et al., 2008; Yagi et al., 2007), we next asked whether *Tead4* is required for *Cdx2* expression even if *Oct3/4* expression levels are reduced. We examined the requirement for *Tead4* in inducing *Cdx2* expression after siRNA-mediated knockdown of *Oct3/4*. In control wild-type (EB5) ES cells, *siOct3/4* transfection led to reduced expression of *Oct3/4* and other ES genes, including *Sox2* and *Fgf4* (Figure 1L). Knockdown of *Oct3/4* also led to increased expression of *Cdx2* and other trophoblast genes (Figure 1L). Interestingly, *Oct3/4* knockdown in *Tead4*$^{-/-}$ ES cells (Nishioka et al., 2008) led to essentially the same changes in gene expression as in wild-type ES cells (Figure 1L), indicating that *Tead4* is not required for expression of *Cdx2* and other trophoblast genes as long as *Oct3/4* levels are reduced. However, immediate induction of *Cdx2* by Tead4VP16 in ES cells was not accompanied by a clear reduction of *Oct3/4* at day 1 (Figure 1I), suggesting that Tead4 can induce *Cdx2* expression by overcoming Oct3/4-mediated suppression. Therefore, in the presence of Oct3/4, Tead4 is required to induce *Cdx2* expression.

Tead4 Regulates *Cdx2* as a Transcriptional Activator In Vivo

These observations suggested that Tead4 can instructively induce *Cdx2* expression and trophoblast fate. However, Tead4 is expressed ubiquitously in preimplantation embryos (Nishioka et al., 2008), raising the question as to how its activity is restricted to outer cells of the nascent TE. We hypothesized that Tead4 activity must be regulated along the inside/outside axis. To test this hypothesis, we first examined the ability of variant forms of Tead4 to induce Cdx2 expression in inside cells when overexpressed. During normal development, Cdx2 is initially ubiquitously expressed and becomes progressively downregulated in inside cells and upregulated in outside cells during blastocyst formation (Ralston and Rossant, 2008). Because levels of Cdx2 are highly variable among embryos and among inside cells of individual embryos during this process (Dietrich and Hiiragi, 2007; Ralston and Rossant, 2008), we examined populations of embryos in which these constructs were ubiquitously overexpressed by RNA injection from the 2-cell stage (Figure 2A).

At the 20- to 30-cell stages, embryos were classified into three phenotypic categories, depending on the level of Cdx2 expression detected in inside cells. That is, type I embryos exhibited undetectable levels of Cdx2 in inside cells, type II embryos exhibited low levels of Cdx2 relative to outside cells, and type III embryos exhibited high levels of Cdx2 (comparable to outside cell levels). At this stage, the majority of water or *β-globin* mRNA-injected embryos exhibited either no Cdx2 (type I) or weak Cdx2 expression (type II) in inside cells, whereas only 8% of embryos on average exhibited strong Cdx2 expression (type III) in a few inside cells (Figures 2C and 2E; see Figure S1 available online). Expression of either full-length Tead4 or a repressor-modified form of Tead4, Tead4EnR (a fusion between the Tead4 containing the DNA-binding domain and the repression domain of *Drosophila* Engrailed), did not lead to changes in Cdx2 expression (Figures 2B and 2E). In contrast, overexpression of Tead4VP16 led to a significant increase in the number of type III embryos exhibiting elevated Cdx2 expression in inside cells (Figures 2B, 2D, and 2E), consistent with our observations in ES cells. The number of inside cells expressing high levels of Cdx2 also increased after Tead4VP16 overexpression (Figure 2D; Figure S1). Injection of higher doses of Tead4VP16 RNA led to increased lethality (not shown). By contrast, overexpression of an unrelated transcription factor fused to the VP16 activation domain (Foxa2VP16) did not affect Cdx2 expression (Figure 2E).

Taken together, these results suggest that the Cdx2-inducing activity of Tead4 is dependent on the presence of an exogenous activation domain. Preimplantation embryos also express *Tead1* and *Tead2* (Nishioka et al., 2008), and these factors are known to bind similar DNA motifs as Tead4 (Sawada et al., 2008). Interestingly, overexpression of activator-modified Tead1 (Tead1VP16) also increased the frequency of type III embryos (Figure 2E), raising the possibility that other Tead proteins may participate in regulation of Cdx2 expression during embryogenesis.

Nuclear Localization of Yap Anticipates Cdx2 Expression in the Outer Cells

Our analyses of constitutively active Tead4 both in ES cells and in the early embryo suggested that Tead4 activity is regulated along the inside/outside axis of the embryo. Tead proteins are known to act in conjunction with the coactivator protein Yap (Vassilev et al., 2001), whose nuclear localization is regulated by phosphorylation (Zhao et al., 2007). *Yap* mRNA was detected throughout preimplantation development by RT-PCR (Figure 3A), prompting us to examine the localization of Yap protein throughout preimplantation development. During

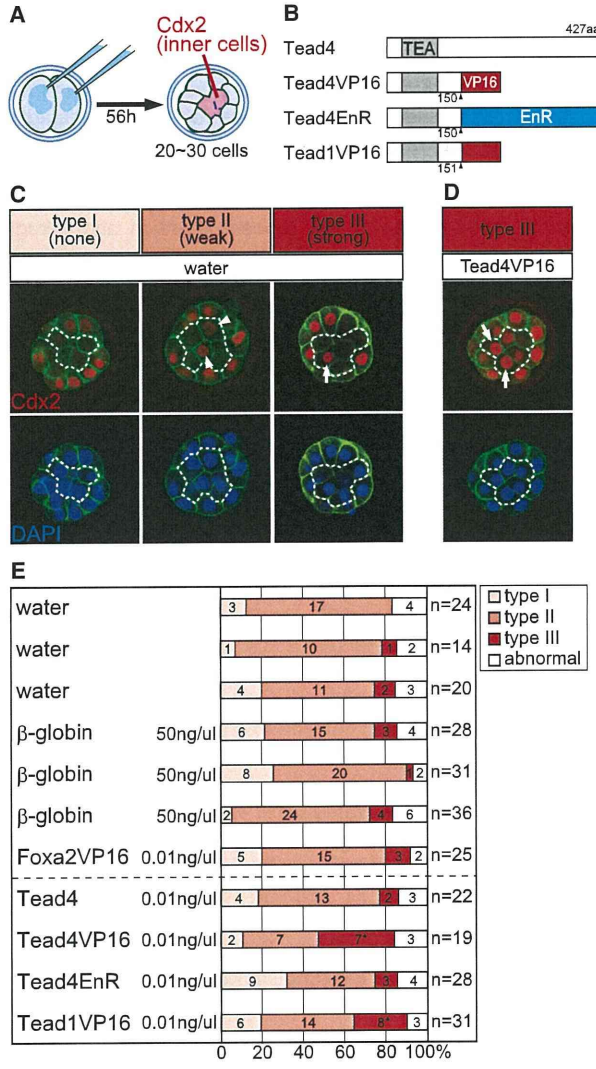

Figure 2. Tead4 Instructively Regulates Cdx2 Expression in Embryos

(A) Scheme for RNA injection for the experiments shown in this figure and Figures 4 and 6. Expression of Cdx2 was examined in inside cells after 56 hr of culture.

(B) Tead variants used in this study.

(C) Examples of three classes of water-injected embryos exhibiting different levels of Cdx2 (red) in inside cells (indicated by a dotted line). Inside cells were identified based on Z-series confocal images of embryos stained with nuclei (DAPI, blue) and cell membranes (β-catenin, green). Inside cells exhibited weak (arrowheads) or strong (arrow) Cdx2 expression.

(D) A representative embryo injected with *Tead4VP16* RNA.

(E) Graph summarizing the effects of *Tead* RNA injection on Cdx2 expression in inside cells. Numbers in each column represent the number of embryos in each category. Asterisks indicate that the differences were statistically significant compared to the *β-globin* RNA-injected group ($p < 0.05$).

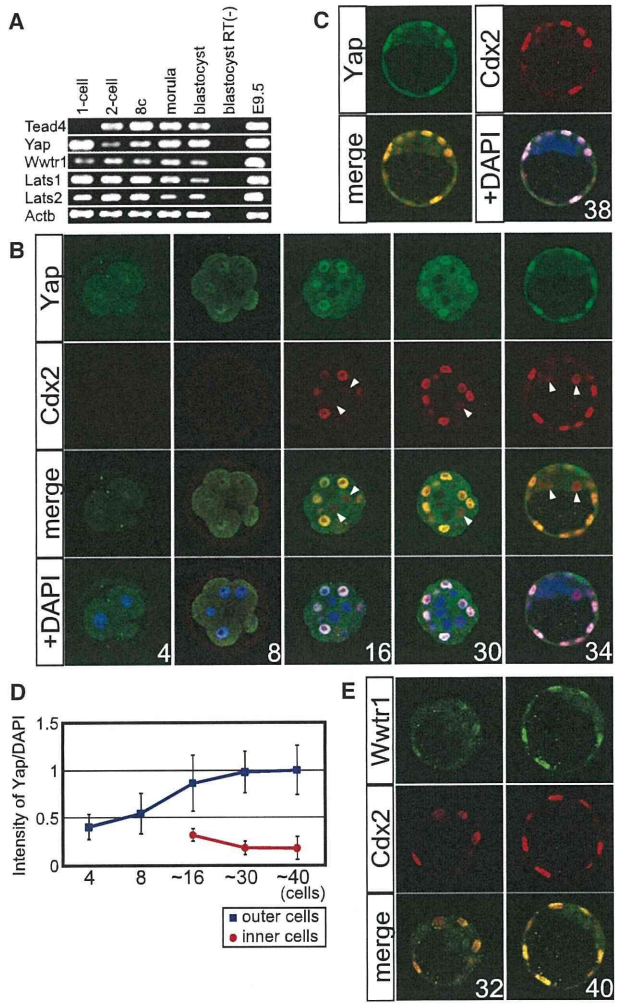

Figure 3. Nuclear Yap Anticipates Outer Cell-Restricted Expression of Cdx2

(A) RT-PCR analysis of gene expression in pools of 50 embryos for each stage indicated.

(B) Immunofluorescence localization of Cdx2 and Yap proteins during preimplantation development. Cdx2 is still detected in some inside cells, although Yap is not (arrowheads).

(C) Yap and Cdx2 localization in nuclei of the TE in the mid/late blastocyst.

(D) Levels of nuclear Yap proteins during preimplantation development. To account for changes in fluorescence due to changing focal planes, Yap fluorescence levels were normalized to corresponding DAPI fluorescence levels for each nucleus.

(E) Immunofluorescence localization of Wwtr1. Embryo cell number is indicated in (B), (C), and (E).

development, nuclear Yap was first detected in embryos at the 4-cell stage, although the signal was weak and variable among embryos and among individual blastomeres (Figure 3B and data not shown). By the early 8-cell stage, nuclear Yap was detected in all blastomeres, even in embryos that had not yet undergone compaction (n = 22) (Figure 3B). After the 8-cell stage, levels of nuclear Yap increased in outside cells up to the 30-cell stage and remained constant thereafter, whereas nuclear Yap decreased in inside cells and Yap appeared to be excluded from the nuclei (Figures 3B and 3D). At the mid/late blastocyst stage, nuclear Yap was restricted to outside cells of the TE and was not detected within cells of the ICM (Figure 3C).

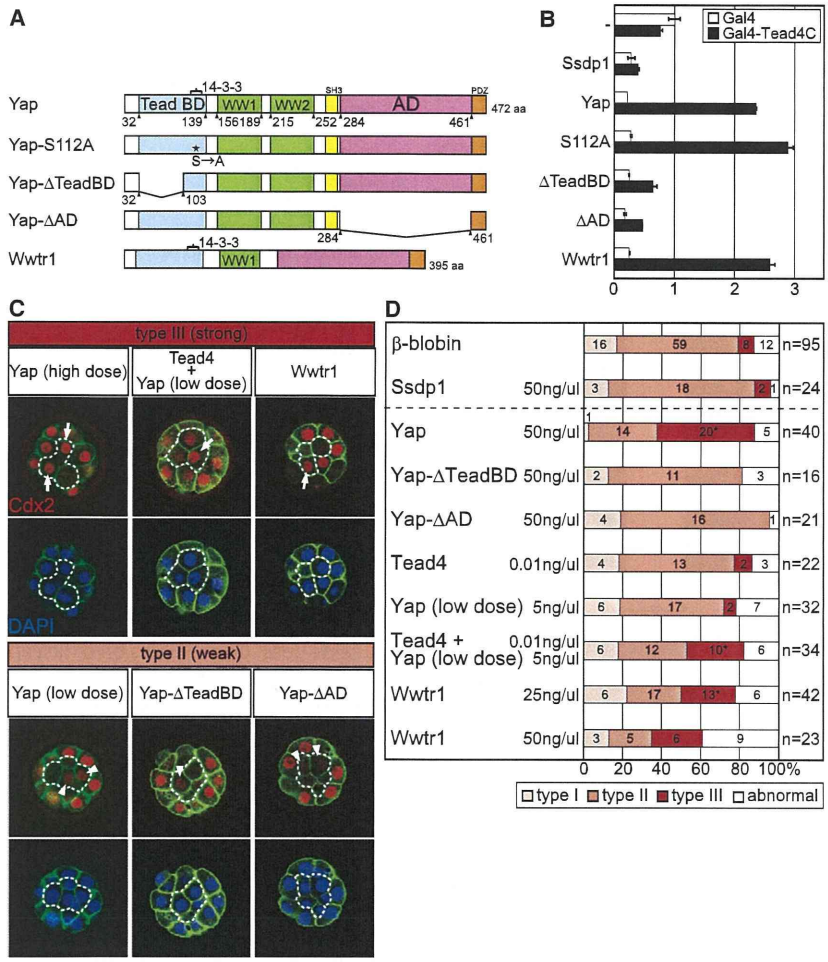

Figure 4. Nuclear Yap Regulates Cdx2 Expression

(A) Yap variants used in this study (TeadBD, Tead-binding domain; WW1 and WW2, WW domains; AD, activation domain; 14-3-3, 14-3-3-binding site; SH3, SH3-binding site; PDZ, PDZ domain-binding site). Residue numbers within the Yap protein were indicated. The domain structure of Wwtr1 was defined based on sequence homology to Yap.

(B) Effects of Yap variants on the transcription activity of Gal4-Tead4C in NIH 3T3 cells.

(C) Representative embryos showing the effects of overexpression of Yap variants on Cdx2 (red) levels. Membrane (green) and nuclei (blue) are also shown.

(D) Graph summarizing the effects of Yap variants on Cdx2 levels in inside cells. The asterisks indicate that the differences were significant compared to the *β-globin* RNA-injected group.

Since *Cdx2* expression begins after compaction around the 8-cell stage (Ralston and Rossant, 2008), nuclear localization of Yap appears to precede expression of Cdx2. In addition, restriction of Yap to outside cells appears to precede that of Cdx2, since nuclear Yap was restricted to outside cells from the 16-cell stage onward, whereas Cdx2 is not clearly restricted to outside cells until later stages (Figure 3B) (Dietrich and Hiiragi, 2007; Niwa et al., 2005; Ralston and Rossant, 2008). Thus, restriction of Yap to outside cell nuclei precedes restriction of Cdx2 expression to outside cells, suggesting that Yap could play a role in Tead4-mediated patterning of Cdx2 expression along the inside/outside axis during blastocyst formation.

Yap and Wwtr1 Regulate Cdx2 Expression in Preimplantation Embryos

We next asked whether Yap could induce Cdx2 expression in inside cells of the embryo. Importantly, Yap cooperatively increased transcription induced by Gal4-Tead4C (a fusion protein of the DNA-binding domain of yeast Gal4 and the C-terminal cofactor-binding domain of Tead4) in NIH 3T3 cells (Figure 4B), confirming the ability of Yap to enhance Tead4-mediated transcriptional activity. Next, *Yap* mRNA was injected into both blastomeres of the 2-cell embryo, and phenotypes were categorized as described above. Overexpression of *Yap* led to a significant increase in the frequency of type III embryos exhibiting high levels of Cdx2 in inside cells (Figures 4C and 4D). In contrast, neither Yap-ΔTeadBD, lacking the Tead binding domain, nor Yap-ΔAD, lacking the transactivation domain, were able to enhance Tead4-mediated transactivation in NIH 3T3 cells (Figures 4A and 4B), and both constructs failed to increase Cdx2 expression in embryos (Figures 4C and 4D). Thus, Yap activity may depend on interaction with Tead. Overexpression of an unrelated coactivator protein, Ssdp1 (Nishioka et al., 2005), had no effect on Tead4-mediated transcription in NIH 3T3 cells, or on Cdx2 expression in embryos (Figures 4B and 4D), confirming the specificity of our observations. Finally, to examine whether Yap can confer Cdx2-inducing ability on unmodified Tead4 (lacking VP16), we examined the ability of unmodified Tead4 to induce Cdx2 expression in the presence of Yap. Injection of either full-length *Tead4* mRNA or low-dose (5 ng/μl) *Yap* mRNA alone had no effect on Cdx2 expression, whereas their coinjection significantly increased Cdx2 expression (Figures 4C and 4D). Taken together, our observations suggest that Yap can induce *Cdx2* expression cooperatively with Tead4.

Although Yap is sufficient to upregulate Cdx2 in inside cells, $Yap^{-/-}$ mutant embryos exhibit normal TE development (Morin-Kensicki et al., 2006). This observation suggested that a Yap-related protein could compensate for the absence of *Yap* during early development. We therefore examined the Yap-related protein Wwtr1 (TAZ) (Mahoney et al., 2005). *Wwtr1* was detected in preimplantation embryos; high levels of Wwtr1 protein were detected in outside cell nuclei (Figures 3A and 3E), whereas low, but detectable, levels of Wwtr1 were detected in inside cell nuclei. Importantly, overexpression of *Wwtr1* was sufficient to increase Cdx2 expression in inside cells (Figures

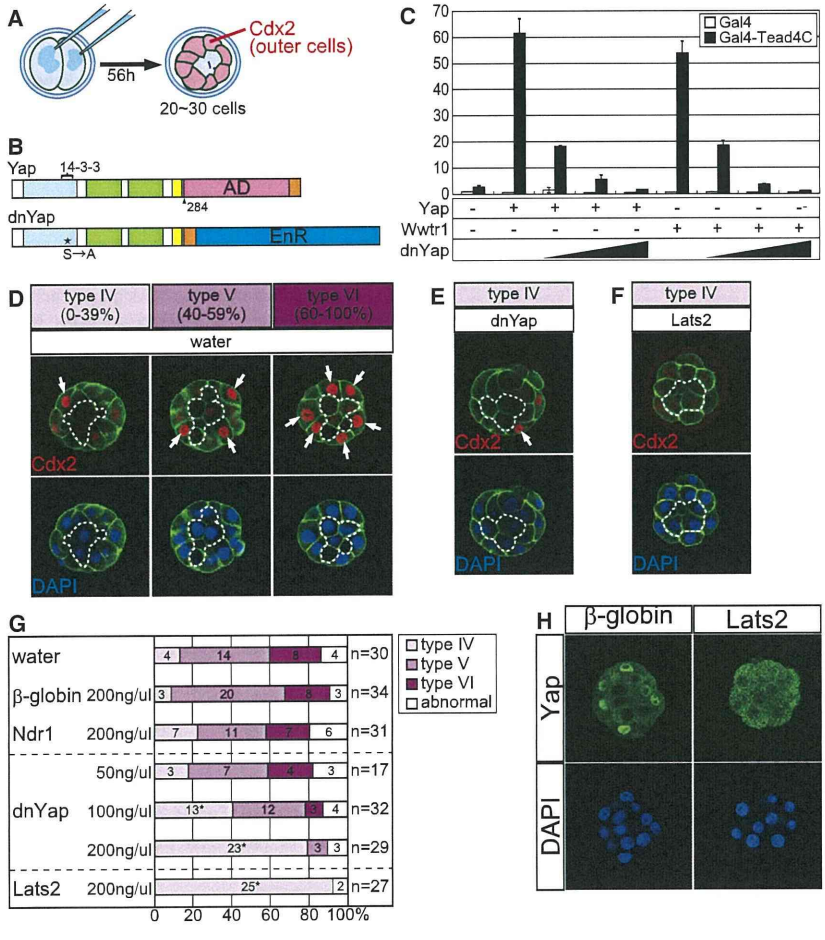

Figure 5. Requirements of Nuclear Yap/Wwtr1 in Cdx2 Expression

(A) Scheme for RNA injection and analysis of Cdx2 in outside cells after 56 hr of culture.

(B) Schematic representation of the structure of dnYap.

(C) Luciferase assay after overexpression of dnYap in HeLa cells.

(D) Examples of embryos classified according to the number of outside cells with strong Cdx2 (red, arrows). Membrane (green) and nuclei (blue) are also shown.

(E and F) Representative embryos injected with (E) *dnYap* or (F) *Lats2* RNA.

(G) Graph summarizing phenotypes resulting from injection of RNAs for *dnYap* or *Lats2* on expression of Cdx2 in outside cells. The asterisks indicate that the differences were significant compared to the control β-globin-injected group.

(H) Effects of *Lats2* RNA injection on subcellular localization of Yap proteins.

4C and 4D), consistent with the hypothesis that Wwtr1 plays a Yap-like role in the early embryo.

Next, we tested the requirement for *Yap* and *Wwtr1* in Cdx2 expression in early embryos. Whereas loss of either *Yap* or *Wwtr1* alone does not lead to abnormalities in preimplantation development (Hossain et al., 2007; Makita et al., 2008; Morin-Kensicki et al., 2006), $Yap^{-/-}$;$Wwtr1^{-/-}$ embryos died before the morula stage (16–32 cells), prior to establishment of inside and outside cell populations (Table S1). Thus, *Yap* and *Wwtr1* are required prior to lineage specification, precluding analysis of their requirement during lineage specification. However, use of a dominant-negative Yap (dnYAP), allowed us to address this issue.

To create dnYap, the transcriptional activation domain of Yap was replaced with the *Drosophila* Engrailed repression domain, and Yap-S112 was converted to A (equivalent to human YAP-S127A) (Figure 5B). Phosphorylation of Yap-S112 by the protein kinase Lats promotes cytoplasmic localization of Yap through interaction with the cytoplasmic scaffold protein 14-3-3 (Basu et al., 2003; Dong et al., 2007; Zhao et al., 2007). In HeLa cells, dnYap strongly suppressed activation of Tead4 by either Yap or Wwtr1 (Figure 5C), confirming the dominant-negative activity of this construct. Next, we overexpressed *dnYap* in embryos by RNA injection as described above, and we examined Cdx2 expression (Figure 5A), with the prediction that dominant-negative Yap would decrease Cdx2 expression in outside cells. Overexpression of dnYap did not cause early lethality, but did alter Cdx2 expression in early blastocysts. Embryos were classified into three categories, based on the fraction of outside cells exhibiting high levels of nuclear Cdx2: embryos exhibiting Cdx2 in 0%–39% of outside cells (type IV), in 40%–59% of outside cells (type V), and in 60%–100% of outside cells (type VI) (Figure 5D). Overexpression of *dnYap* RNA significantly increased the frequency of type IV, while decreasing the frequency of type V and type VI embryos in a dose-dependent manner (Figures 5E and 5G). Thus, dnYap decreased expression of Cdx2 in outside cells, and regulation of Cdx2 expression appears to be dependent on Tead4 coactivator activity. These results are consistent with the hypothesis that Yap and Wwtr1 act together with Tead4 to regulate Cdx2 expression in outside cells during blastocyst formation. In addition, other domains of Yap/Wwtr1 proteins may be required for viability at very early stages.

Lats Regulates Yap Localization during Preimplantation Development

We next sought to examine how Yap becomes localized to nuclei of outside cells prior to TE formation. In cultured cells, Lats1/2-mediated phosphorylation of Yap/Wwtr1 leads to their cytoplasmic localization (Dong et al., 2007; Hao et al., 2008; Lei et al., 2008; Zhang et al., 2008a; Zhao et al., 2007). We therefore examined the localization of phosphorylated Yap (p-Yap) by using an antibody raised against p-Yap. Prior to the blastocyst stage, p-Yap was detected in the cytoplasm of inside cells, and at the blastocyst stage high levels of cytoplasmic p-Yap were detected within ICM cells (Figure 6A). Protein phosphatase treatment of embryos eliminated this pattern (Figure 6A, right), confirming the specificity of the antibody. These observations